Geology of the Red Mountain Mining District, Esmeralda County, Nevada

GEOLOGICAL SURVEY BULLETIN 1423

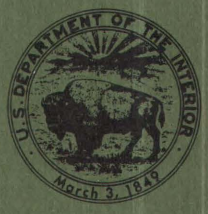

Geology of the Red Mountain Mining District, Esmeralda County, Nevada

By W. J. KEITH

GEOLOGICAL SURVEY BULLETIN 1423

UNITED STATES GOVERNMENT PRINTING OFFICE, WASHINGTON : 1977

UNITED STATES DEPARTMENT OF THE INTERIOR

GEOLOGICAL SURVEY

V. E. McKelvey, *Director*

Library of Congress Cataloging in Publication Data

Keith, William J. 1933-
Geology of the Red Mountain mining district, Esmeralda County, Nevada

(Geological Survey Bulletin 1423)
Bibliography: p. 43-45
Supt. of Docs. No.: I 19.3:1423
1. Geology, Stratigraphic-Miocene. 2. Volcanic ash, tuff, etc.-Nevada-Esmeralda Co. 3. Geology-Nevada-Esmeralda Co. I. Title. II. Series: United States Geological Survey Bulletin 1423
QE75.B9 no. 1423 [QE694] 557.3'08s [557.93'35] 76-608325

For sale by the Superintendent of Documents, U. S. Government Printing Office
Washington, D. C. 20402

Stock Number 024-001-02948-1

CONTENTS

ILLUSTRATIONS

TABLES

GEOLOGY OF THE RED MOUNTAIN MINING DISTRICT, ESMERALDA COUNTY, NEVADA

By W. J. KEITH

ABSTRACT

The Red Mountain mining district is in the central part of the Silver Peak Range near the west-central boundary of the Basin and Range province, approximately 14 km west-southwest of the town of Silver Peak, Esmeralda County, Nev. The district consists of interlayered volcanic flows, breccias, and tuffs, and sedimentary rocks all of which are Miocene in age. The volcanic rocks form a continuous differentiation series that is alkali-calcic in composition. Structures in the district are predominantly high-angle northeast-trending normal faults that formed in response to subsidence. Many of these faults were mineralized near the end of Miocene time to form sheeted quartz-calcite fissure veins that contain both precious and base metals. The district has produced mainly silver and gold with minor amounts of lead, zinc, and copper.

INTRODUCTION

The area covered by this report is near the west-central boundary of the Basin and Range province (Fenneman, 1931). It is an east-west strip approximately 8 km long and 3 km wide on the crest and east flank of the Silver Peak Range that includes the larger mines of the Red Mountain mining district about 14 km west-southwest of the town of Silver Peak, Esmeralda County, Nev. (fig. 1). The Nivloc mine is at the east end of the district and the Mohawk (Argentite) mine at the west end. The district is readily accessible on the east end by a gravel road leading from Silver Peak through the ghost town of Nivloc to the Sixteen-To-One mine. Many poorly maintained roads extend north and south from the main road. Access to the west end is gained by driving south from the town of Silver Peak to Lower Cowcamp Springs, then northwest to the crest of the range, a distance of about 40–50 km. Much of this road lies in dry washes and for part of the year is impassable to all but four-wheel-drive vehicles.

Climate in the area is arid or locally semiarid. The average rainfall ranges from less than 120 mm at Dyer, Nev. (U. S. Weather Bur., 1965), to more than 300 mm at altitudes above 2 km. Springs are scattered throughout the area, but few flow year round. The vegetation in the lower elevations consists mainly of a sparse cover of sage and some greasewood near Clayton Valley. The higher elevations are

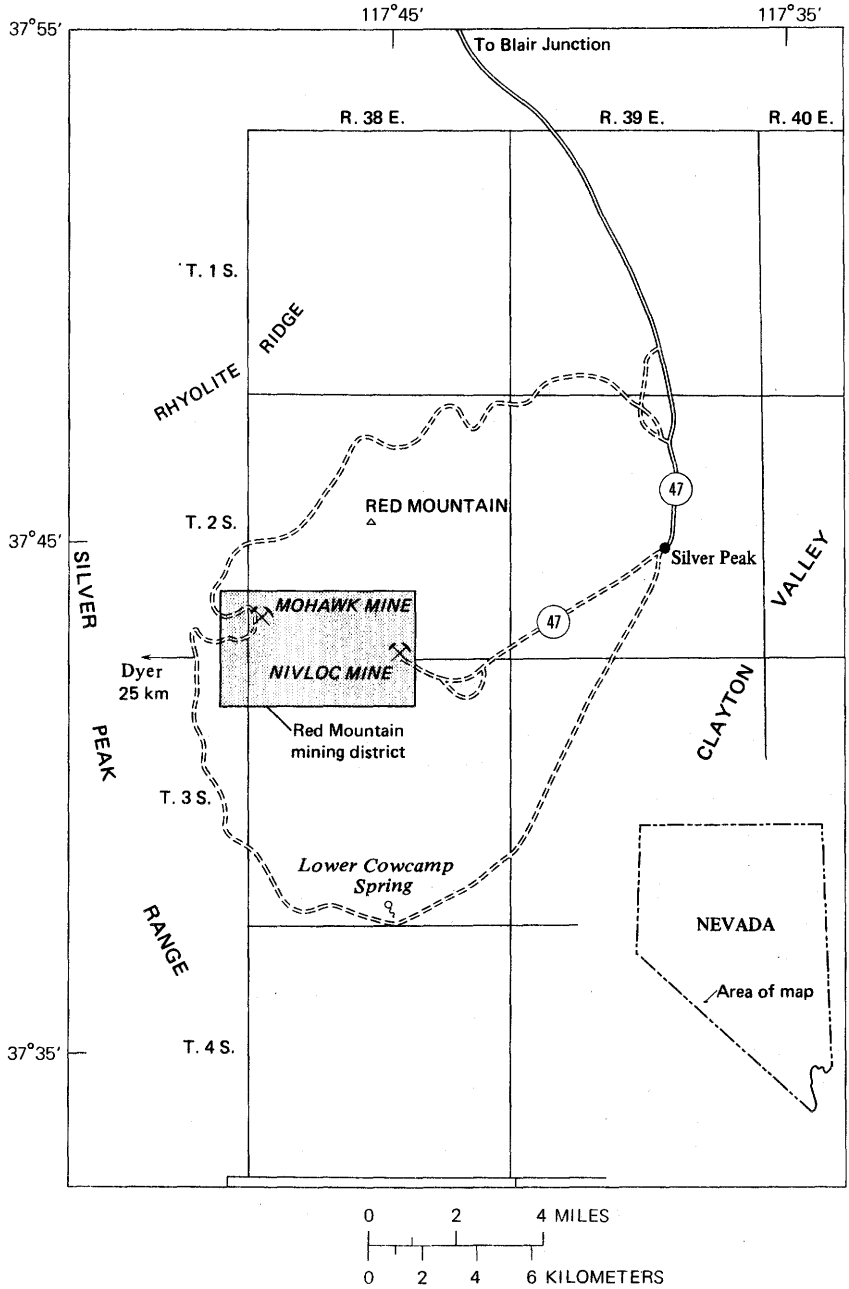

FIGURE 1.—Map of Silver Peak Range showing Red Mountain mining district.

sparsely covered by pinon pine and juniper. Springs and streams are usually lined with a thick growth of willow and rose. Small clumps of

cottonwood trees grow where springs are large enough to support them.

The Red Mountain mining district is on the east flank of the Silver Peak Range, which forms the west margin of a natural amphitheater. The south and east margins of the amphitheater are the Palmetto Mountains and Clayton Ridge, respectively. The district has a rugged topography and ranges in elevation from 1,600 to 2,700 m. The west third of the district is marked by a northeast-trending ridge that acts as a divide. Drainage on the east side trends east to southeast and is rather deeply entrenched. Drainage on the west side of the divide trends west to southwest and is markedly less entrenched.

PREVIOUS WORK

Almost all prior information on the Red Mountain mining district pertains to regional geology. The only detailed work available is a geologic map of the central part of the Silver Peak Range at a scale of 1:48,000 and a fairly detailed description of the Cenozoic stratigraphy and structure (Robinson, 1964).

The earliest work in the district was by Turner (1900a, b; 1902; 1909), who produced a 1:125,000-scale geologic map of the Silver Peak quadrangle and named the Esmeralda Formation. Spurr (1903) included the area in his reconnaissance study of Nevada south of the 40th parallel.

More recent work in the district began with Bailly (1951) who briefly described the Nivloc mine (fig. 1) and the veins in the Coyote mine, which is a few kilometers northeast of the Nivloc mine. Robinson augmented his 1964 report with reports on the Silver Peak collapse caldera (1968), the petrology of the volcanic center (1972), and the stratigraphy of the entire Silver Peak region (Robinson and others, 1968).

A brief description of the Red Mountain district is included in the mineral resource report of Esmeralda County by Albers and Stewart (1972). Other recent reports list geochemical data and sample descriptions from the Sixteen-To-One mine access tunnel (Ashley and Keith, 1971) and contain a preliminary geologic map of the district (Keith, 1972).

FIELDWORK AND ACKNOWLEDGMENTS

Approximately 9 months were spent in the field during the summers of 1968 through 1971. The geology was mapped on aerial photographs at a scale of 1:8,000 and transferred to a topographic base. The access tunnel and the main crosscut in the Sixteen-To-One mine were mapped by R. P. Ashley and the author in 1968 (Ashley and Keith, 1971). The remainder of the underground work was completed by the author in 1971 assisted by Duncan Foley.

I wish to acknowledge the assistance of R. P. Ashley and S. C. Creasey of the U. S. Geological Survey for their aid in field interpretations and of R. L. Rose of San Jose State University for discussions of and suggestions for solving many of the geologic problems that arose. Midcontinent Mining Co. and Sunshine Mining Co. kindly granted permission to work in the Sixteen-To-One mine.

Thanks are due to the people of the town of Silver Peak for their friendship and for information on the area. Special thanks are given to Mr. and Mrs. Alva Zunich for their continued aid and encouragement; Mr. Zunich kindly supplied information on underground exploration in the area.

GEOLOGY

The Red Mountain mining district is entirely within the Silver Peak volcanic center and is characterized largely by volcanic rocks of late Miocene age. The volcanic center is bounded on all sides by rocks of Cambrian age (Albers and Stewart, 1972), and Ordovician rocks occur near the south edge of the center (McKee, 1968). Sedimentary rocks of presumably Paleozoic age have been found below 91 m in the Nivloc mine. A major hiatus representing Ordovician to Jurassic time exists in the geologic record in this area. Granitic rocks of Jurassic age were intruded into Paleozoic sedimentary rocks all around the volcanic center (Albers and Stewart, 1972).

The oldest rocks exposed at the surface in the district are sedimentary breccia of fanglomeratic origin composed largely of Paleozoic rock fragments. Fine-grained lake sediments were deposited with angular discordance on the breccia and were subsequently tilted.

After this period of sedimentation, a series of major volcanic eruptions produced thick sequences of andesitic to rhyolitic lava flows that are interbedded with water-laid sediments and a few air-fall and ash-flow tuffs. Extrusion of the lavas caused subsidence that produced high-angle normal faults. The eruptions lasted almost until the end of the Miocene Epoch at which time some of the fault zones were mineralized by fluids probably related to the same igneous source that produced the lavas.

The district was probably under continual uplift from Miocene through Pliocene time because there is no evidence of any deposition during this time interval. The older gravels in the district may be as old as Pleistocene, but most, or possibly all, are Holocene. All of the gravels are being dissected at present, indicating recent uplift of the area.

The only known structures produced in the district since the end of Miocene time are a few north-trending Basin and Range faults.

SEDIMENTARY BRECCIA

The oldest exposed rock in the volcanic-sedimentary complex is a

sedimentary breccia, which is limited to the east half of the mining district (pl. 1) and unconformably overlies Paleozoic rocks north of the district (Robinson, 1964). A camel bone found near the base of the breccia by Robinson was identified as either *Megatylopus* sp. or *Aepycamelus* sp. by S. David Webb (Robinson and others, 1968, p. 606). The vertebrate mammalian stage indicated is probably Hemphillian, Clarendonian, or Barstovian.

The sedimentary breccia unit, which is more than 1,500 m thick (Robinson and others, 1968), displays very little relief and consists mostly of low rounded hills and deeply entrenched washes. Its color ranges from pale purple to green. It is composed mainly of poorly sorted, poorly bedded angular fragments of Paleozoic rocks from surrounding areas and a matrix of small angular rock fragments cemented with calcite and (or) clay minerals. Large clasts (9–12 m long) of pencil slate (probably Harkless Formation) occur locally. The upper part of the unit consists mainly of well-sorted brown sandstone and pebble conglomerate composed of volcanic detritus which is, at most, a few meters thick. Some of the fragments are as large as 60 cm in diameter, but generally they are about 5 cm.

The angularity of the fragments and the poor sorting and bedding in most of the unit suggest a very short distance of transport. These features, along with the heterogeneity of the unit, are characteristic of a fanglomerate. The sandstone and conglomerate at the top are better sorted, display numerous cut-and-fill structures, and locally show graded bedding.

SANDSTONE AND CONGLOMERATE

A unit of sandstone and conglomerate also is confined to the east half of the district (pl. 1) and is about 183 m thick. It unconformably overlies the sedimentary breccia and locally contains lenses of sedimentary breccia. These lenses contain fragments of the breccia as well as individual Paleozoic rock fragments and generally display better sorting than the breccia unit and well-defined crossbedding. Much of the section (siltstone, sandstone, and shale) was probably deposited in lake waters as indicated by fine-grained sediments and horizontal bedding. The unit has been discontinuously silicified, which indicates either that solutions entered the unit in more than one place or that existing silica was remobilized. Field evidence suggests that part of the silicification was due to intrusion of rhyolitic plugs.

The sandstone conglomerate unit consists of siltstone, sandstone, pebble conglomerate, limy shale, and locally boulder conglomerate. The sandstone and conglomerate range in color from buff or pink to green, whereas the limy shale is black to gray or buff. The boulder conglomerate and some of the pebble conglomerate contain lithic fragments of the sedimentary breccia unit.

The detritus forming this unit is composed of pyroclastic debris that includes crystal fragments of quartz, K-feldspar (usually sanidine), plagioclase, biotite, altered glass shards, and subrounded to subangular lithic fragments of shale, sandstone, siltstone, and minor chert. Some buff limy siltstone contains small amounts of ostracod shells and possible plant remains.

ANDESITE

Andesite unconformably overlies the sandstone-conglomerate unit and crops out mainly in the central part of the mining district, although good exposures occur near the west edge of the district. Drill hole data (A. Baker, 3d, unpub. geol. rept.) indicate a thickness of more than 245 m for this unit in the vicinity of Sixteen-To-One Canyon.

Chemical analyses of these rocks (table 1) show a high concentration of Al_2O_3 and MgO in the porphyritic subunits due to a concentration of plagioclase and olivine phenocrysts in the rocks.

LOWER PORPHYRITIC ANDESITE

The lower part of the andesite unit is composed of flows of porphyritic andesite that unconformably overlie the sedimentary conglomerate unit. Locally this unit has been brecciated and recemented with aphanitic andesitic lava. It is generally slightly altered but locally displays intense hydrothermal alteration.

The flow rocks are composed of phenocrysts of plagioclase, olivine, and pyroxene set in an intergranular groundmass. The size of phenocrysts varies greatly. Maximum dimensions for plagioclase, olivine, and pyroxene phenocrysts are 2, 3, and 4 mm, respectively. The groundmass is composed of plagioclase laths, interstitial ferromagnesian and opaque minerals (clinopyroxene and magnetite), and anhedral plagioclase. Some of the specimens contain in the groundmass a large amount (estimated at 3–4 percent) of penninite(?), which appears to be an alteration product of glassy parts of the groundmass.

Plagioclase is mainly labradorite (An_{44-63}) (Tröger, 1952, p. 113) with good albite and Carlsbad twinning. Most crystals are subhedral, and some show synneusis textures (fig. 2) similar to those described by Vance (1969). Forsteritic olivine (table 2) occurring as subhedral to anhedral phenocrysts is the dominant ferromagnesian mineral. The composition is about Fo_{89} on the basis of X-ray crystallographic data applied to the forsterite determinative curves of Jackson (1960). The olivine, which has a positive $2V$ of about 80°, is generally partly altered to smectite (nontronite?) and magnetite. The smectite ranges

from greenish yellow to olive green and is generally fine grained and platy.

Clinopyroxene phenocrysts ($2V_z=55°$) are euhedral to subhedral augite and commonly display twinning and zoning. They generally occur in monomineralic clusters. Locally, the pyroxene has been partly altered to a smectite mineral, similar in appearance to that found as replacement of the olivine phenocrysts.

The groundmass consists of plagioclase, augite (pigeonite?), lesser amounts of orthopyroxene(?), and magnetite, with an intergranular fabric. The plagioclase laths range in composition from An_{32} to An_{50} and constitute one of two distinct phases of plagioclase crystallization in the groundmass. The second phase consists of anhedral untwinned plagioclase filling the interstices between the plagioclase laths, pyroxene, and magnetite. Most of the pyroxene in the groundmass is fresh and appears to be augite, although a smaller amount of what appears to be orthopyroxene has been altered to chlorite. Most of the chlorite, however, formed as an alteration product of glass in the groundmass.

Analyses of representative samples from this unit indicate a normative plagioclase composition of about An_{60} (samples 100 and 318, table 1), which agrees with the phenocryst composition (table 2). Sample 100, with 0.4 percent normative quartz (table 1), is close to the silica saturation boundary, and sample 318, with 5.7 percent normative olivine, is moderately undersaturated.

The high alumina content reflects the large percentage of plagioclase phenocrysts in the rocks (table 2, samples 100 and 318). These high-alumina andesites are probably the result of the accumulation of plagioclase crystals through crystal fractionation. This type of andesite is generally considered to be a type of accumulate rather than a primary magma type (Yoder and Tilley, 1962, p. 354).

The magnesia content of these rocks can be accounted for by noting the presence of the olivine and pyroxene in the modal analyses. Sample 318 has a high percentage of magnesia (6.2 percent, table 1) relative to sample 100 (3.7 percent, table 1) and also a higher percentage of modal olivine (6.3 percent, table 2); part of the magnesia in sample 100 is present in chlorite (penninite?) in the groundmass.

LOWER ANDESITIC SEDIMENTARY ROCKS

Exposures of the lower andesitic sedimentary rocks, which consist of sandstone and conglomerate, are limited to the south side of Sixteen-To-One Canyon. Exposures of the andesitic sedimentary rock in the mining district other than in Sixteen-To-One Canyon are included in the undivided andesite unit. The lower andesitic sedimentary rock conformably overlies the lower porphyritic andesite and is

TABLE 1.—*Analyses, in percent, of volcanic rocks in the central Silver Peak Range, Nev.*

[Chemical analyses by rapid-rock method: Analysts; Lowell Artis, S.D. Botts, Gillison Chloe, P.L.D. Elmore, J. L. Glenn, James Kelsey, Roosevelt Moore, and Hezekiah Smith. Semiquantitative spectrographic analyses by Harry Bastron and Chris Heropoulos. Results are reported in percent to the nearest number in a series 1, 0.7, 0.5, 0.3, 0.2, 0.15, and so on, which represent approximate midpoints of interval data on a geometric scale. The assigned interval for semiquantitative results will include the quantitative value for about 30 percent of the results. Looked for but not found: Ag, As, Au, Bi, Cd, Ge, Hf, Hg, In, Li, Pd, Pt, Re, Sb, Ta, Te, Th, Tl, U, W, Zn, Pr, Sm, and Eu]

Sample No.	305	318	100	269	301	60	178	317	122B	17	313	122A	126	170	127
Plotting[1] symbol	○	○	○	○	○	●	●	○	●	●	○	●	●	●	●
Chemical analyses															
SiO_2	44.80	47.20	47.40	48.10	48.20	48.92	49.16	53.50	53.52	54.06	54.70	54.80	55.17	56.79	58.95
Al_2O_3	22.40	18.30	20.40	18.20	20.00	16.54	15.39	15.50	17.24	16.76	16.10	17.16	16.74	17.86	17.69
Fe_2O_3	6.80	2.60	4.40	3.60	4.30	4.95	6.37	2.00	4.62	2.54	3.80	3.81	3.80	4.45	3.83
FeO	2.40	5.40	4.00	3.90	4.00	3.51	2.89	4.20	2.51	4.32	2.40	2.74	3.00	1.89	1.53
MgO	2.50	6.20	3.70	5.30	3.90	6.78	7.26	4.50	4.15	5.79	5.20	3.98	3.97	2.47	1.61
CaO	10.00	9.80	9.70	9.10	9.80	8.55	7.94	7.70	6.78	7.48	4.30	6.55	6.97	5.71	4.65
Na_2O	3.00	2.50	3.00	3.00	2.90	3.44	3.11	2.00	3.81	3.58	3.50	3.64	3.44	4.14	4.29
K_2O	1.40	1.50	1.60	1.90	1.80	2.62	2.37	2.10	3.39	3.19	3.40	3.46	3.16	3.58	4.19
H_2O+	2.20	2.80	1.80	2.10	1.70	1.60	2.04	3.00	.87	.55	2.90	1.59	.98	.57	.81
H_2O-	.62	.70	.82	2.10	.66	.50	.81	.71	.66	.05	1.40	.27	.65	.53	.89
TiO_2	1.60	1.20	1.40	1.40	1.50	1.49	1.54	1.00	1.24	.96	1.00	1.04	1.12	1.16	1.05
P_2O_5	.84	.61	1.00	.69	1.00	.68	.56	.39	.65	.37	.41	.57	.60	.45	.37
MnO	.22	.14	.21	.23	.14	.13	.16	.10	.08	.12	.10	.11	.10	.09	.10
CO_2	1.10	.76	.14	.08	------	------	------	3.20	------	------	1.20	------	------	------	------
Total	99.88	99.71	99.57	99.70	99.90	99.71	99.60	99.90	99.52	99.77	100.41	99.72	99.70	99.69	99.96
CIPW norms[2]															
Q	------	------	0.437	------	1.022	------	------	12.340	1.581	------	5.927	3.776	5.805	5.697	7.642
C	------	------	------	------	------	------	------	------	------	------	------	------	------	------	------
or	8.621	9.286	9.766	11.767	10.905	15.861	14.475	13.345	20.443	19.008	21.169	20.893	19.041	21.458	25.198
ab	26.454	22.163	26.222	26.604	25.158	27.871	27.200	18.199	32.900	30.546	31.204	31.474	29.681	35.533	36.944
an	45.352	35.915	38.706	32.051	37.152	22.489	21.740	29.158	20.336	20.410	19.153	20.708	21.314	19.856	16.932
ne	------	------	------	------	------	1.056	------	------	------	------	------	------	------	------	------
wo	.262	4.528	1.776	4.400	2.503	6.854	6.343	3.834	4.032	6.084	.209	3.629	4.153	2.461	1.706
en	4.184	10.459	9.519	10.893	9.958	5.887	14.957	12.052	10.548	10.446	13.645	10.129	10.082	6.240	4.081
fs	------	4.096	1.848	1.901	1.616	.048	------	4.941	------	3.240	------	.379	.720	------	------
fo	1.615	4.007	------	2.061	------	7.997	2.615	------	------	2.869	------	------	------	------	------
fa	------	1.729	------	.396	------	.072	------	------	------	.981	------	------	------	------	------
mt	3.977	3.949	6.590	5.470	6.392	7.353	5.554	3.118	4.854	3.714	5.440	5.645	5.618	3.066	2.254
hm	4.344	------	------	------	------	------	2.754	------	1.367	------	.252	------	------	2.399	2.344
il	3.167	2.388	2.747	2.787	2.921	2.899	3.023	2.042	2.403	1.839	2.001	2.018	2.169	2.235	2.029
tn	------	------	------	------	------	------	------	------	------	------	------	------	------	------	------
ru	------	------	------	------	------	------	------	------	------	------	------	------	------	------	------
ap	2.073	1.514	2.447	1.713	2.428	1.650	1.371	.993	1.571	.884	1.023	1.380	1.449	1.081	.892
Total	100.048	100.035	100.056	100.040	100.055	100.038	100.032	100.023	100.035	100.021	100.024	100.031	100.033	100.025	100.021

Salic	80.427	67.364	75.131	70.421	74.237	67.278	63.415	73.042	75.260	69.964	77.453	76.851	75.841	82.543	86.716
Femic	19.621	32.670	24.925	29.620	25.817	32.759	36.616	26.981	24.775	30.056	22.570	23.180	24.192	17.481	13.305

Partitions

di	0.489	8.724	3.372	8.342	4.740	12.789	11.825	7.395	7.516	11.658	0.390	6.793	7.801	4.588	3.180
di, wo	.262	4.528	1.776	4.400	2.503	6.854	6.343	3.834	4.032	6.084	.209	3.629	4.153	2.461	1.706
di, en	.227	3.015	1.337	3.357	1.925	5.887	5.482	2.525	3.485	4.254	.181	3.050	3.405	2.127	1.474
di, fs	------	1.181	.260	.586	.312	.048	------	1.035	------	1.319	------	.114	.243	------	------
hy	3.957	10.359	9.770	8.851	9.336	------	9.475	13.433	7.063	8.113	13.464	7.344	7.154	4.113	2.607
hy, en	3.957	7.444	8.181	7.536	8.033	------	9.475	9.527	7.063	6.192	13.464	7.079	6.677	4.113	2.607
hy, fs	------	2.915	1.588	1.315	1.304	------	------	3.906	------	1.920	------	.265	.477	------	------
ol	1.615	5.737	------	2.457	------	8.069	2.615	------	------	3.850	------	------	------	------	------
ol, fo	1.615	4.007	------	2.061	------	7.997	2.615	------	------	2.869	------	------	------	------	------
ol, fa	------	1.729	------	.396	------	.072	------	------	------	.981	------	------	------	------	------
wol	------	------	------	------	------	------	------	------	------	------	------	------	------	------	------

Rittmann numbers and rock names[3]

k	+0.24	+0.26	+0.28	+0.30	+0.29			+0.41			+0.39				
an	+.55	+.50	+.52	+.44	+.49			+.46			+.25				

Semiquantitative spectrographic analyses

B	------	------	------	------	0.0007	------	------	------	------	------	------	------	0.001	------	0.0007
Ba	0.15	0.15	0.15	0.10	.15	0.15	0.1	0.05	0.15	0.15	0.07	0.15	.1	0.15	.15
Be	.0002	------	------	------	------	.00015	------	.0001	.0003	.0002	------	.0002	------	.0002	.0005
Ce	.015	------	------	------	------	.01	.015	------	.01	.01	.01	------	.01	.015	.01
Co	.002	.003	.002	.003	.002	.005	.003	.002	.002	.003	.002	.002	.003	.002	.0015
Cr	.005	.03	.005	.03	.005	.02	.03	.03	.01	.02	.02	.007	.01	.002	.0015
Cu	.003	.005	.002	.007	.003	.005	.007	.003	.005	.007	.005	.002	.007	.005	.003
Ga	.002	.0015	.002	.002	.0015	.0015	.0015	.0015	.0015	.002	.002	.0015	.0015	.002	.002
La	.007	.007	.007	.007	.007	.005	.007	------	.007	.007	.005	.005	.005	.005	.005
Mo	------	------	------	------	.0005	------	------	------	------	------	------	------	------	.0003	.0002
Nb	.001	.0007	.0007	.0007	.001	.0015	.0015	.001	.0015	.0015	.001	.001	.001	.0015	.0015
Ni	.003	.015	.0015	.02	.0015	.02	.02	.007	.01	.01	.015	.005	.007	.002	.001
Pb	.001	------	------	------	.001	.001	.0015	.001	.005	.0015	.003	.0015	.002	.002	.002
Sc	.002	.002	.0015	.003	.002	.003	.003	.002	.002	.003	.002	.0015	.002	.0015	.0015
Sr	.2	.15	.2	.15	.2	.15	.15	.2	.15	.15	.1	.15	.15	.15	.1
V	.02	.015	.02	.02	.02	.02	.02	.015	.015	.02	.015	.015	.015	.015	.01
Y	.003	.0015	.002	.003	.002	.003	.003	.002	.003	.003	.003	.002	.003	.003	.003
Yb	.0003	.0002	.0002	.0003	.0002	.0003	.0003	.0002	.0003	.0003	.0003	.0003	.0003	.0003	.0003
Zr	.015	.015	.015	.015	.015	.03	.03	.01	.03	.03	.015	.03	.03	.03	.05

See footnotes at end of table.

TABLE 1.—*Analyses, in percent, of volcanic rocks in the central Silver Peak Range, Nev.*—Continued

Sample No.	99	339	130	287	131	9	369	219	53	482	279	117	479	483	OB
Plotting[1] symbol	●	○	●	○	●	●	○	●	●	○	○	●	○	○	●
Chemical analyses															
SiO_2	59.70	60.40	60.78	61.60	61.75	63.17	63.50	63.79	66.19	70.80	71.50	73.38	73.60	75.40	75.96
Al_2O_3	16.90	17.00	16.80	15.40	16.85	16.49	16.90	16.49	16.23	13.50	14.30	13.32	13.60	13.30	13.08
Fe_2O_3	4.40	3.00	3.58	2.70	4.46	3.13	2.90	3.54	2.31	1.30	1.70	1.14	1.40	.73	.39
FeO	1.10	1.30	1.58	.76	.54	1.05	.52	.36	.62	.76	.40	.25	.72	.20	.45
MgO	2.30	1.20	2.22	.54	1.33	1.15	1.40	1.09	.51	.38	.44	.16	.32	.09	.13
CaO	4.40	3.20	4.18	4.10	3.49	3.18	2.50	2.73	1.56	1.60	.92	.97	.92	.48	.71
Na_2O	3.80	3.80	4.18	4.80	4.53	4.42	3.90	4.40	4.86	3.00	3.50	3.75	3.20	2.50	3.87
K_2O	3.60	5.00	4.23	5.20	4.51	4.83	5.10	4.94	5.66	5.60	5.30	4.98	5.30	5.80	4.69
H_2O+	1.50	1.80	.40	1.20	.59	.57	1.20	.72	.54	2.40	1.00	.80	.52	1.00	.22
H_2O-	.43	.34	.18	.21	.40	.41	.59	.39	.28	.11	.66	.54	.13	.24	.01
TiO_2	1.00	.92	1.01	.71	.90	.84	.69	.76	.66	.39	.38	.26	.33	.21	.12
P_2O_5	.57	.37	.40	.29	.38	.34	.31	.26	.16	.12	.14	.03	.12	.07	.02
MnO	.08	.07	.06	.10	.12	.10	.08	.11	.10	.14	.10	.11	.14	.10	.06
CO_2	----	1.40	----	2.70	----	----	.32	----	----	.08	.06	----	.18	.02	----
Total	99.78	99.80	99.60	100.31	99.85	99.68	99.91	99.58	99.68	100.18	100.40	99.69	100.48	100.14	99.71
CIPW norms[2]															
Q	12.848	12.010	10.004	8.198	10.413	12.141	15.060	13.007	12.960	29.032	29.010	30.785	32.709	38.124	33.828
C	.120	.420	-----	-----	-----	-----	1.187	-----	-----	-----	1.488	.070	1.218	2.229	.396
or	21.741	30.694	25.244	31.942	26.958	28.918	30.815	29.645	33.832	33.909	31.738	29.922	31.429	34.662	27.859
ab	32.861	33.404	35.720	42.221	38.774	37.893	33.743	37.810	41.598	26.012	30.012	32.264	27.173	21.394	32.918
an	18.502	13.981	14.729	5.319	12.465	11.033	10.611	10.820	5.820	7.000	3.698	4.694	3.793	1.946	3.409
ne	-----	-----	-----	-----	-----	-----	-----	-----	-----	-----	-----	-----	-----	-----	-----
wo	-----	-----	1.492	5.785	.818	1.127	-----	.157	.397	.138	-----	-----	-----	-----	-----
en	5.854	3.105	5.584	1.398	3.351	2.902	3.565	2.757	1.285	.970	1.110	.405	.800	.227	.325
fs	-----	-----	-----	-----	-----	-----	-----	-----	-----	-----	-----	-----	-----	-----	.420
fo	-----	-----	-----	-----	-----	-----	-----	-----	-----	-----	-----	-----	-----	-----	-----
fa	-----	-----	-----	-----	-----	-----	-----	-----	-----	-----	-----	-----	-----	-----	-----
mt	.928	1.820	2.384	.747	-----	1.293	-----	-----	.417	1.820	.521	.418	1.827	.366	.568
hm	3.857	1.861	1.971	2.292	4.511	2.280	2.965	3.595	2.049	.077	1.363	.871	.145	.486	-----
il	1.941	1.815	1.937	1.402	1.413	1.616	1.298	1.011	1.268	.759	.731	.502	.629	.403	.229
tn	-----	-----	-----	-----	.408	-----	-----	.588	-----	-----	-----	-----	-----	-----	-----
ru	-----	-----	-----	-----	-----	-----	.022	-----	-----	-----	-----	-----	-----	-----	-----
ap	1.380	.910	.957	.714	.910	.816	.751	.625	.383	.291	.336	.072	.285	.168	.048
Total	100.031	100.021	100.022	100.017	100.021	100.019	100.017	100.015	100.010	100.008	100.009	100.003	100.008	100.005	100.002
Salic	86.072	90.509	85.696	87.680	88.610	89.985	91.416	91.282	94.211	95.953	95.946	97.735	96.322	98.355	98.411
Femic	13.959	9.512	14.325	12.337	11.411	10.034	8.601	8.732	5.799	4.055	4.062	2.268	3.686	1.650	1.590
Partitions															
di	------	------	2.782	3.016	1.524	2.102	------	.292	.740	.257	------	------	------	------	------
di, wo	------	------	1.492	1.618	.818	1.127	------	.157	.397	.138	------	------	------	------	------

di, en	------	------	1.290	1.398	.707	.974	------	.135	.343	.119	------	------	------	------	------
di, fs	------	------	------	------	------	------	------	------	------	------	------	------	------	------	------
hy	5.854	3.105	4.294	------	2.644	1.927	3.565	2.621	.942	.851	1.110	.405	.800	.227	.745
hy, en	5.854	3.105	4.294	------	2.644	1.927	3.565	2.621	.942	.851	1.110	.405	.800	.227	.325
hy, fs	------	------	------	------	------	------	------	------	------	------	------	------	------	------	.420
ol	------	------	------	------	------	------	------	------	------	------	------	------	------	------	------
ol, fo	------	------	------	------	------	------	------	------	------	------	------	------	------	------	------
ol, fa	------	------	------	------	------	------	------	------	------	------	------	------	------	------	------
wol	------	------	------	4.167	------	------	------	------	------	------	------	------	------	------	------

Rittmann numbers and rock names[3]

k		+0.47		+0.42			+0.46			+0.55	+0.50		+0.52	+0.61	
an		+.18		+.06			+.16			+.09	+.10		+.10	+.11	

Semiquantitative spectrographic analyses

B	0.002	------	0.0015	------	0.001	0.001	0.0007	0.001	0.0015	0.003	------	0.005	------	0.001	0.003
Ba	.15	0.2	.15	0.15	.15	.15	.2	.15	.15	.02	0.02	.02	0.02	.015	.016
Be	.0002	.0002	.0003	.00015	.0003	.0005	.00015	.0003	.0003	.0005	.0005	.0005	.0005	.0003	.0004
Ce	.015	------	.015	.02	.015	.015	------	.015	.01	.015	.01	------	.015	.01	------
Co	.0015	.0007	.002	.0005	.0015	.001	.0003	.0007	------	.0002	.0002	------	.0002	------	------
Cr	.003	.0007	.003	.0007	.002	.0015	.0003	.0002	------	.0003	.0007	------	.0003	------	.0001
Cu	.003	.0015	.003	.0003	.002	.002	.0005	.0015	.0005	.0002	.0005	.0005	.0015	.00007	.0001
Ga	.002	.003	.002	.0015	.002	.002	.0015	.002	.0015	.002	.002	.0015	.002	.002	.0016
La	.007	.007	.007	.01	.007	.007	.01	.007	.005	.01	.01	.003	.01	.007	.005
Mo	.001	------	.0003	------	.0002	------	------	.0003	------	.0007	------	------	------	------	.0003
Nb	.002	.001	.002	.0015	.002	.002	.0015	.002	.0015	.003	.003	.0015	.003	.002	.002
Ni	.0015	.0003	.003	------	.002	.0015	------	.0002	------	------	------	------	------	------	------
Pb	.002	.002	.003	.003	.003	.003	.003	.003	.003	.003	.005	.003	.005	.003	.003
Sc	.0015	.0015	.001	.0007	.001	.001	.001	.0007	.0007	.0003	.0003	------	.0003	.0002	.0003
Sr	.15	.07	.1	.07	.1	.07	.15	.1	.07	.015	.015	.01	.01	.03	.01
V	.015	.007	.01	.005	.007	.01	.007	.007	.003	.003	.003	.0007	.002	------	.0011
Y	.003	.003	.003	.005	.003	.005	.002	.003	.003	.003	.003	.001	.003	.003	.0009
Yb	.0003	.0003	.0003	.0003	.0003	.0003	.0002	.0003	.0003	.0003	.0003	.00015	.0003	.0002	.0001
Zr	.02	.03	.05	.03	.05	.03	.02	.05	.07	.02	.02	.02	.02	.02	.011

[1]The analyses with the plotting symbol ● are taken from Robinson (1972); ○, this report.

[2]The CIPW norms were calculated assuming no water and no CO_2 using the computer program of Bowen (1972).

[3]The Rittmann numbers and names were derived only for the author's analyses. Rittmann rock names: Samples 305, 318, 100, 301—pigeonite-labradorite-andesite; 269, 317—labradorite-olivine-trachyandesite; 313, 339—latite; 287—alkali trachyte; 369—quartz-latite; 482, 279, 479, 483—rhyolite.

Sample locations are based on the 1,000-m Universal Transverse Mercator grid system, zone 11:

305	4174590.053N	431108.466E	301	4174419.046N	430283.670E	287	4175639.450N	430321.363E	279	4175827.928N	431252.959E
318	4174051.549N	430892.215E	317	4174057.511N	430675.313E	369	4175232.486N	430331.453E	479	4175402.449N	431140.345E
100	4174205.836N	430976.549E	313	4174363.776N	431235.163E	482	4173072.789N	434911.068E	483	4174509.954N	430488.238E
269	4176087.386N	431082.546E	339	4174592.534N	430120.724E						

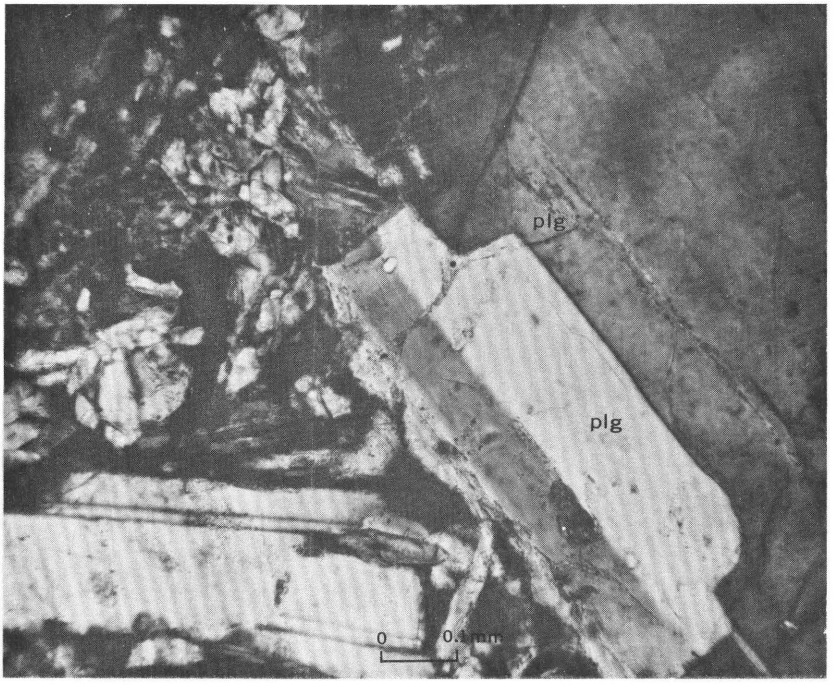

FIGURE 2.—Synneusis texture in plagioclase phenocrysts (plg) in andesite.

composed predominantly of andesite, pumice, and quartz fragments, which give the unit a blue-gray to pale-green color.

The unit is poorly to moderately well sorted, and the lithic and crystal fragments are subangular to subround. Crossbedding in the subunit is rare, and, although minor normal (coarse to fine upward) graded bedding exists, it too is rather uncommon. The individual beds range in thickness from a few centimeters to more than 50 cm, but they are generally less than 10 cm. These features, together with the fact that much, if not all, of the material is locally derived, indicate that the unit was probably formed as a result of the volcanic activity in the Silver Peak volcanic center. Deposition probably took place in a shallow lake or pond.

Along with the andesite, pumice, and quartz, the unit also contains minor amounts of fragmental plagioclase, limestone, and granitic rock. The matrix of this rock is predominantly detrital and appears to consist largely of a fine-grained mixture of illite, kaolinite, and quartz. A small amount of calcite also occurs in the matrix as veinlets and cement.

APHANITIC ANDESITE

The aphanitic andesite consists of fine-grained andesite flows that conformably overlie the lower andesitic sedimentary rocks. A few

TABLE 2.—*Thin-section modes, in percent, of representative volcanic rocks in the Red Mountain mining district*

Sample	Unit	Name	Plagioclase	K-feldspar	Biotite	Amphibole	Olivine	Clino-pyroxene	Quartz	Sphene	Groundmass	
269	a	Labradorite, olivine, trachyandesite.	20.8(An_{38-52})	----------	----------	----------	9.9	2.2	----------	----------	67.1	Intergranular texture, plagioclase (An_{45}), augite, magnetite.
318	lpa	Pigeonite, labradorite, andesite.	25.2(An_{45-53})	----------	----------	----------	6.3	2.3	----------	----------	66.2	Intergranular texture, plagioclase, augite, magnetite.
100	lpa	Pigeonite, labradorite, andesite.	36.7(An_{44-63})	----------	<1	----------<1		----------	----------	----------	62.9	Intergranular texture, plagioclase(An_{32-50}), pigeonite (?), magnetite.
305	upa	Pigeonite, labradorite, andesite.	29.2(An_{57-62})	----------	----------	----------	2.4	----------	----------	----------	68.4	Intergranular texture, plagioclase, augite, magnetite.
301	upa	Pigeonite, labradorite, andesite.	32.5(An_{43-65})	----------	----------	----------	1.1	----------	----------	----------	66.4	Pilotaxitic texture, plagioclase, augite, magnetite.
369	la	Quartz latite ----------	20.4(An_{24-32})	3.5	4.8	----------	----------	<1	----------	----------	70.7	Cryptofelsitic texture, high-K groundmass.
365	la	Biotite, augite, latite ------	21.0(An_{23-24})	5.0	4.1	----------	----------	1.6	----------	----------	68.3	Holohyaline texture.
287	la	Alkali trachyte ----------	17.9(An_{22-28})	3.4	1.8	----------	----------	<1	----------	----------	76.5	Cryptofelsitic texture, high-K groundmass.
482	pr	Rhyolite ----------	10.2(An_{28})	7.9	1.6	----------	<1	----------	1.1	<1	78.6	Holohyaline texture, high-K groundmass.
4	pr	Rhyolite ----------	11.9(An_{26-28})	9.3	2.0	<1	----------	----------	2.9	1.1	72.3	Holohyaline texture, high-K groundmass.
2	pr	Rhyolite ----------	8.2(An_{18-20})	3.9	<1	<1	----------	----------	4.8	<1	81.8	Spherulitic texture, high-K groundmass.
479	prd	Rhyolite ----------	4.0(An_{27-30})	2.9	<1	----------	----------	----------	5.8	----------	86.9	Cryptofelsitic texture, high-K groundmass.
344	prd	Rhyolite ----------	11.7(An_{28-32})	----------	1.9	<1	----------	----------	3.4	----------	82.8	Cryptofelsitic texture, high-K groundmass.
279	prd	Rhyolite ----------	6.0	<1	2.5	<1	----------	----------	2.8	<1	87.8	Cryptofelsitic texture, high-K groundmass.

[1]Names according to Rittmann's (1952) chemical classification (table 1).

pods of black calcareous siltstone mark contacts in an otherwise massive-appearing section of andesite. These pods are generally less than 2.5 m in diameter and less than 25 cm thick, and many contain probable plant remains.

The flows have a pilotaxitic texture and consist of a microcrystalline mat of plagioclase crystals and interstitial orthopyroxene(?) that has been altered to chlorite (penninite?). Scattered sparsely throughout the unit, commonly 15–30 cm apart, are individual xenocrysts of quartz and twinned plagioclase. Quartz is generally round to subround and locally exhibits resorption embayments. Plagioclase also displays some embayment.

The normative anorthite content of the aphanitic andesite as represented by samples 313 and 317 (table 1) is also about An_{60}. The alumina content is distinctively lower than that of the porphyritic andesites (a=15.8 percent, lpa=19.8 percent, samples 313, 317, 100, and 318, table 1). The large percentage of normative quartz (12.3 percent, table 1) in the unit can be explained in part by the presence of the quartz xenocrysts and in part by the presence of groundmass quartz indicated by X-ray diffraction. The magnesia in this unit is represented by a large amount of penninite(?), which is pervasive throughout the groundmass and has also replaced the orthopyroxene.

UPPER ANDESITIC SEDIMENTARY ROCKS

Upper andesitic sedimentary rocks consist of sandstone and conglomerate and are limited to the north side of Sixteen-To-One Canyon. This is not the result of any large dislocation between the north and south sides of the canyon but occurs simply because the lower andesitic sedimentary rocks are covered on the north side of the canyon by volcanic breccia and colluvium. The upper andesitic sedimentary rocks conformably overlie the aphanitic andesite and contain abundant debris derived from it.

The upper andesitic sedimentary rocks, like the lower ones, are the direct result of the tectonic unrest in the Silver Peak volcanic center. The sediments that formed them were water laid and contain minor crossbedding and graded bedding, although there is less bedding of any kind in these rocks than in the lower andesitic sedimentary rocks. The beds that are distinguishable in these rocks tend to be thicker and more massive than those in the lower. The upper unit, like the lower one, is also poorly to moderately sorted and contains subangular to subrounded fragments.

The sandstone and conglomerate of the upper andesitic sedimentary rocks are composed predominantly of fragments of pumice, andesite, and quartz with minor amounts of plagioclase crystals and lithic fragments of limestone and granitic rock. However, the andesitic

fragments in the upper unit are predominantly aphanitic. The matrix of the upper andesitic sedimentary rocks is predominantly detrital; however, calcite is present as a cement and in small amounts as veinlets in and near plagioclase crystal fragments.

UPPER PORPHYRITIC ANDESITE

The upper porphyritic andesite conformably overlies the upper andesitic sedimentary rocks and consists, as do the other volcanic units, of multiple flows. Approximately 2.5 m of basal flow breccia is present locally. The rock is a dense blue-black mass that is only locally altered.

The mineralogical makeup of this rock is similar to the lower porphyritic andesite (table 2). Phenocrysts consist of plagioclase, olivine, and possibly clinopyroxene. The groundmass is pilotaxitic and contains 7–10 percent magnetite, as well as minor amounts of interstitial ferromagnesian minerals in the plagioclase mat.

Plagioclase phenocrysts in this rock have an anorthite content of An_{43-65}, which is slightly higher than that of the older rocks but still within the labradorite compositional range. The plagioclase phenocrysts generally have albite and Carlsbad twinning, and some show compositional zoning. Inclusions of magnetite, ferromagnesian minerals, and apatite are crudely alined parallel to the compositional zoning of the plagioclase phenocrysts. They are more abundant in the plagioclase phenocrysts of this rock than in those of the older andesitic rock.

Olivine phenocrysts are subhedral to anhedral and are considerably more altered than those in the older flows. The phenocrysts are partially to completely altered to a smectite. Some of the smectite pseudomorphs have shapes suggestive of pyroxene crystals.

Chemical analyses of samples 301 and 305 (table 1), which are generally representative of this unit, indicate high alumina (20 to 22.4 percent, table 1) and low magnesia (2.5 to 3.9 percent, table 1) relative to the other andesitic rocks. The modal analyses of the same samples (table 2) indicate a high concentration of plagioclase phenocrysts and a low concentration of olivine, which corresponds to the high percentage of alumina and the low magnesia. The normative anorthite content of the upper porphyritic andesite averages about An_{61} (samples 301 and 305, table 1), which is in good agreement with the plagioclase phenocryst composition (table 2) and also with the other andesitic rocks.

VOLCANIC BRECCIA

Volcanic breccia is generally confined to the central part of the district, although thin patches of it occur in many places in the dis-

trict. The unit reaches thicknesses of more than 152 m in the center of the district and thins towards the north, east, and south. To the west the relative thickness of this unit is unclear because it is covered by latitic rocks. The breccia is interbedded with the upper andesitic rocks and the lower part of the rhyolitic rocks. Contacts between the breccia and andesitic and rhyolitic rocks are sharp, showing no gradation from the lava into the breccia. The contacts range in attitude from horizontal to nearly vertical, indicating that the breccia was deposited over some areas of fairly rugged topography.

Most of the volcanic breccia gives no indication of any bedding or layering. However, bedding (fig. 3), as well as a crude layering (fig. 4) due to a preferred orientation of the clasts, occurs locally at the distal edges of the breccia mass. The bedding shown in figure 3 is similar to basal bedding in lahars described by Schmincke (1967).

The volcanic breccia is heterolithologic and varies greatly in composition in single outcrops. It is extremely poorly sorted and contains lithic fragments composed predominantly of andesite and rhyolite, a few pumice fragments, and Paleozoic rock fragments. The matrix generally consists of an aggregate of small (5 mm–<0.2 mm) rock and crystal fragments, and local areas contain glass shards and spherulites. Very few of the larger fragments (>6.4 mm), some of which

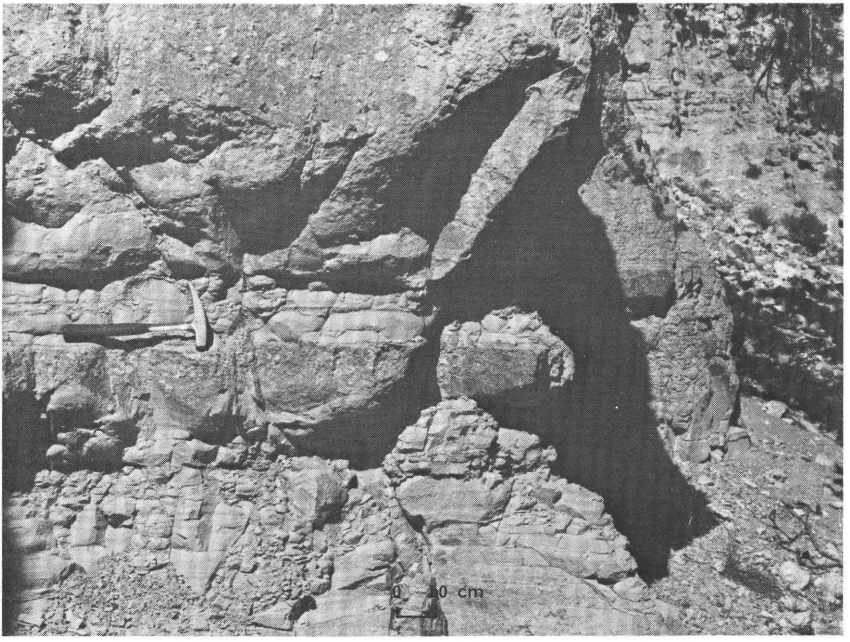

FIGURE 3.—Siltstone and graded beds near the base of the volcanic breccia.

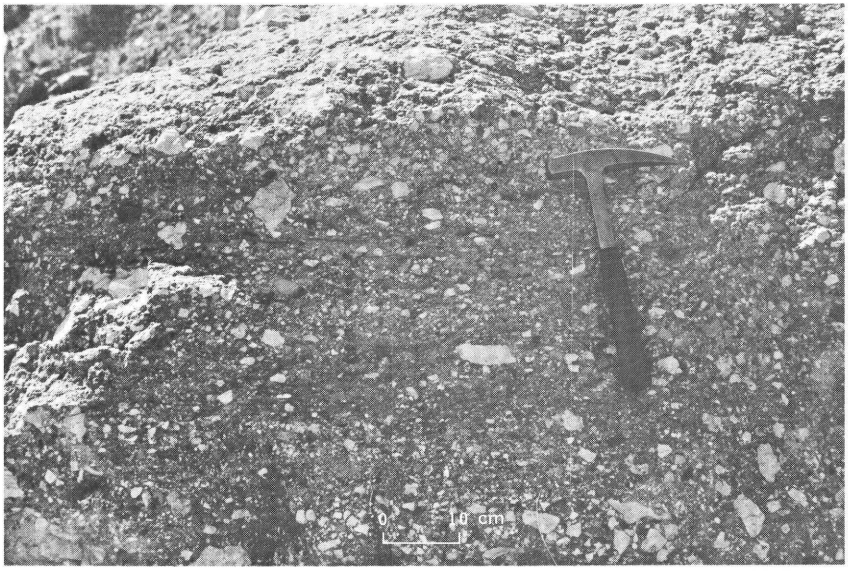

FIGURE 4.—Crude layering in the volcanic breccia.

reach 9 m or more in diameter, touch each other. Many of the outcrops display breccia dikes as much as 1 m wide (fig. 5).

Structural features and lithologic heterogeneity of the unit indicate a complex origin rather than deposition from a single event (Curtis, 1954; Durrell, 1944; Fischer, 1960; Parsons, 1968). The bulk of the unit is probably laharic in origin, and local areas are related to vent breccias.

RHYOLITIC ROCKS

Rhyolitic rocks are quite widespread, occurring in almost all parts of the district except for the extreme north and south sections of the west half. The rocks are thickest in the west-central part of the district, where they reach a maximum thickness of over 180 m.

The rhyolite wedges out toward the east, unconformably overlies the andesitic rocks, and is interlayered with the volcanic breccia. It consists of pale blue-green to buff rhyolitic flows and tuffs, flow breccias, and, locally, fine-grained rhyolitic intrusive rocks. Where possible, the intrusive rhyolite and the rhyolite tuff were mapped as separate cartographic units. The rhyolite tends to form cliffs and steep slopes and, in general, appears very rugged. Locally, remnants of flows and intrusive plugs form jagged spires.

Rhyolitic flows are generally aphanitic to cryptocrystalline and commonly display well-developed perlitic fractures. X-ray diffractograms indicate that quartz and alkali feldspar are the dominant min-

FIGURE 5.—Dike of volcanic breccia (vb) cutting andesitic rocks (a).

erals. Staining of the rocks with cobaltinitrite indicates the presence of a substantial amount of potassium feldspar.

The tuffs, which are predominantly ash-flow tuffs, are composed of pumice fragments, lithic fragments, partly resorbed quartz crystals, and, in many places, lithophysae as much as 25 cm in diameter. The size and quantity of the lithophysae appear to vary randomly laterally, but they are generally confined to the lower part of the tuffs.

Microscopically, a few of the tuffs have a plumose texture that probably indicates devitrification of the glass in a welded section. Some samples also exhibit microgranular masses of alkali feldspar, and randomly oriented biotite occurs locally with alkali feldspar in the interstices. Most quartz phenocrysts found in the tuffs are euhedral. The lithophysae are composed of intergrown alkali feldspar and cristobalite and form a concentric structure.

The normative composition of a representative sample (483, table 1) from this unit indicates that K-feldspar is 59 percent of the total feldspar. The sample also contains 2.23 percent normative corundum (table 1). Normative corundum is not uncommon in rocks of this general composition (Nockolds, 1954), but the amount in this sample

is rather large. This is due to the excess of alumina over what can be used by CaO, K_2O, and Na_2O in the normative calculations.

INTRUSIVE RHYOLITE

Intrusive rhyolite occurs as plugs and dikes throughout the district, but they are generally too small (1–2 m) to be shown on the map. A few of the larger bodies of intrusive rhyolite are shown on the map.

The rhyolite intrudes all previously described units, as well as some of the other rhyolitic flows and tuffs. The strike of the flow banding in the intrusive rhyolite is random, but dips consistently range from 65° to 90°. Many are porphyritic and contain phenocrysts(?) of biotite. Xenocrystic(?) graniticlike clots of quartz and feldspar are common, as well as xenoliths of andesitic rocks. The groundmass is generally cryptocrystalline and consists of quartz and alkali-feldspar as determined by X-ray diffraction.

RHYOLITE TUFF

Outcrops of rhyolite tuff that are large enough to map as a separate unit are confined to the central part of the district (pl. 2). The outcrops consist of irregularly interlayered crystal and lithic air-fall tuffs. The crystal tuffs are usually quite thin (6 cm) and are composed predominantly of quartz crystals. The lithic tuffs, which range in color from pale pink to pale green, are generally more massive than the crystal tuffs and are as much as 3 m thick. They are composed predominantly of fragments of pumice and volcanic rock. Most of the layers appear to have a crude preferred orientation of the crystals and lithic fragments.

Thin beds (as much as 3 cm thick) of tuffaceous sandstone are sporadically interbedded with the crystal and lithic tuffs. The sandstone is moderately well sorted and locally shows crossbedding or normal graded bedding. These features indicate that the tuffs were sporadically reworked by water between eruptions.

SANDSTONE AND SHALE

Most of the sandstone and shale is confined to the northeast one-quarter of the mining district (pl. 1), where it reaches a maximum thickness of 91 m. A few outcrops occur in the southeast quarter, but these are relatively thin. The sandstone and shale unit, which unconformably overlies the rhyolitic rocks, is a small apparently isolated basin deposit composed of interbedded shale, sandstone, and pebble conglomerate, limestone lenses, shale, and lapilli tuff.

The different lithologies in the unit form multicolored outcrops. The interbedded section ranges from brown to pale green and consists

mainly of sandstone and pebble conglomerate, which are composed of volcanic rock fragments, crystal fragments, and smaller amounts of Paleozoic rock fragments. The relative amounts of each lithology randomly vary laterally as well as vertically. The limestone lenses are seldom more than 2 m wide, are gray black, and generally contain small plant(?) fragments. They are scattered throughout the section and probably represent small stagnant isolated ponds. The shale ranges from pink to buff, is tuffaceous to calcareous in composition, and is locally silicified. Where the shale is silicified and has been weathered, the edges tend to expand and separate leaving gaps between partings. The air-fall lapilli tuff, which caps the unit, is white to pale green and latitic in composition and has anorthoclase as the alkali feldspar. The lapilli are rather uniform in size (25 mm) and generally slightly elongate.

LATITIC ROCKS

Latitic rocks are concentrated in the east and west thirds and in the southern part of the district (pl. 1). Minor exposures have also been mapped in the northern part of the central third. This unit is the most widespread and is second only to the sedimentary breccia in thickness (290+ m). The latitic rocks which were dated by the K-Ar method at 5.9±0.2 m.y. (million years) (Robinson and others, 1968), form the youngest volcanic unit in the district. Stratigraphically, they disconformably overlie the sandstone and shale.

The latitic rocks are composed of latitic tuffaceous sedimentary rocks, lava flows, and dikes. Individual specimens are classified as latite, trachyte, quartz latite, and rhyolite. They are closely related stratigraphically and spatially, however, and have been placed in a single group to emphasize these relations; because latitic rocks form the bulk of this unit, the term is applied to the whole group. On the basis of mineralogy, mode of emplacement, and spatial relations, the latitic rocks have been subdivided into latite dikes, latitic tuffaceous sedimentary rocks, latitic flows and tuffs, porphyritic rhyolite flows (pl. 1), and a porphyritic rhyolite dike. These lithologies are discussed separately to explain the stratigraphy.

LATITIC TUFFACEOUS SEDIMENTARY ROCKS

Latitic tuffaceous sedimentary rocks are exposed at the base of the latitic flows in the west-central part of the district. They disconformably overlie the sandstone and shale (pl. 1) and range in thickness from a few centimeters to more than 30 m. The tuffaceous sedimentary rocks are composed largely of a pale-green waterlaid tuff that grades upward into a massive air-fall crystal tuff. Interbedded in this are thin (3 cm–1.8 m) layers of black calcareous shale. The waterlaid tuff usually exhibits graded bedding; no crossbedding was observed. The

upper part of the unit is generally more massive in appearance than the lower. The tuff is composed of feldspar, clinopyroxene, iron ore, glass shards, pumice, and sparse rhyolitic fragments.

The interbedded shale is composed of cryptocrystalline quartz, calcite, and a magnesium-rich chlorite, which was identified by X-ray diffraction. The calcite appears to be concentrated in thin (1 mm) beds in the shale, which alternate with the beds containing the mixture of chlorite and quartz.

LATITE DIKES

Latite dikes form a poorly defined northeast-trending band in the north-central part of the district (pl. 1). The dikes display crosscutting relations with both the rhyolitic and andesitic rocks and are therefore younger. They are most likely contemporaneous with the latitic tuffaceous sedimentary rocks. The dikes, which dip steeply, are gray to pale green. They generally are pervasively hydrothermally altered, but relict textures and minerals indicate that the unaltered rock consisted of phenocrysts of plagioclase, augite, and hornblende (partially altered to biotite) all set in a pilotaxitic groundmass. The plagioclase is altered to calcite and fine-grained mica, and the original composition cannot be determined. Whole-rock alteration is of the potassic type and introduced illite-sericite and adularia.

Hydrothermal alteration of these rocks is illustrated by the chemical analysis of sample 339 (table 1), which is representative of the area. The high SiO_2 content is reflected in the 12 percent normative quartz; the leaching of the CaO and introduction of K_2O and Na_2O are reflected in the low lime and high alkali values. Staining the rocks with an aqueous solution of cobaltinitrite indicates the presence of a substantial amount of K_2O in the groundmass. This is probably the adularia which is indicated by X-ray diffractograms.

LATITE

Latite, which reaches a thickness of more than 183 m, forms a continuous cover over almost the entire west one-third of the district (pl. 1), mostly in the southern part. This unit, which consists of both tuffs and lava flows, conformably overlies the latitic sedimentary rocks, and locally appears to grade into them. The individual flows and tuffs are petrographically similar and were therefore mapped as a single unit. The latite tends to form flat or gently rolling hills except at the edges of the exposures, where it forms cliffs that usually display good columnar jointing. The latite is generally purple, except where hydrothermally altered. The altered areas range from red in the moderately altered areas to white in the areas of more intense alteration and leaching.

The latite is mostly porphyritic and contains sporadic glomeropor-

phyritic clots of plagioclase and interstitial augite and hematite. Phenocrysts consist of augite, biotite, sanidine, orthoclase, and plagioclase, which ranges in composition from oligoclase to andesine (An_{22-38}). Some of the plagioclase phenocrysts have a spongy texture owing to abundant glass inclusions (fig. 6). Sanidine has a negative $2V$ of approximately 5° and ranges from euhedral crystals to anhedral angular fragments. Orthoclase has a negative $2V$ of approximately 70°. Neither the orthoclase nor sanidine displays any twinning. Together they constitute about 14 percent of the phenocrysts (table 2).

The groundmass is composed of a mat of plagioclase laths in a pilotaxitic texture, although it is cryptocrystalline (possibly devitrified glass) in some thin sections. It contains small amounts of magnetite and clinopyroxene, sporadic zircons, and long slender apatite crystals, as much as 0.3 mm long.

The latite, like the latite dikes, is pervasively hydrothermally altered. The alteration is generally potassic, with the introduction of K-feldspar (adularia) and K-mica (illite-sericite). Alteration is not constant throughout the unit, however, but varies in intensity and also in the amount of removal and addition of major elements. In

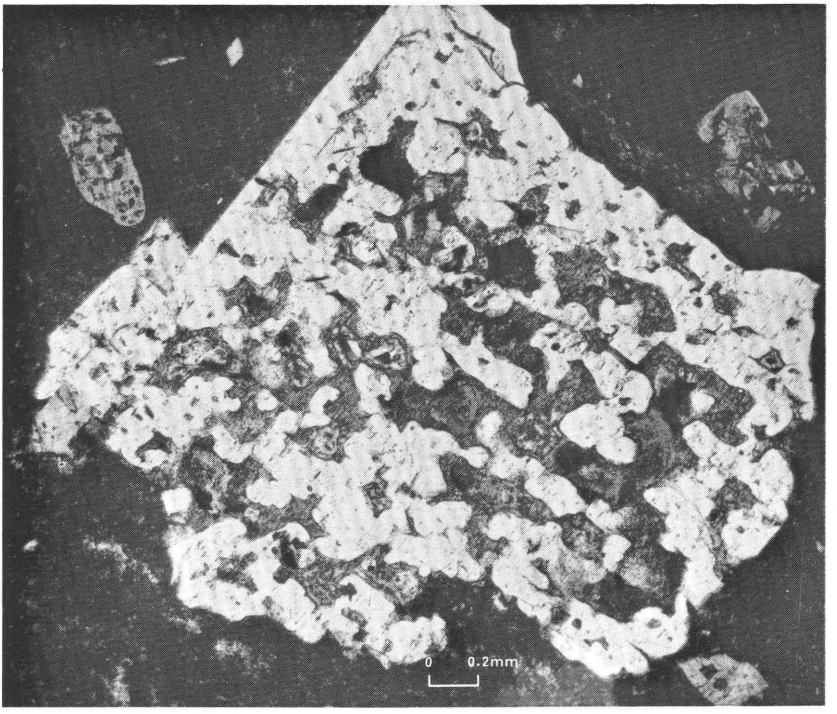

FIGURE 6—Sponge texture in plagioclase phenocrysts in latite.

some areas alteration is mainly propylitic with the formation of chlorite. In others, there are silicified zones where SiO_2 has replaced almost everything in the rocks. The chemical analyses of samples 287 and 369 (table 1), like analyses of the latite dikes, indicate an excess of K_2O and Na_2O and a deficiency in CaO relative to what would be expected for latite. Both the samples also contain excess SiO_2, which probably indicates light silicification along with potassic alteration.

PORPHYRITIC RHYOLITE FLOWS

Porphyritic rhyolite flows, which are generally red to gray, conformably overlie the latite and form the youngest unit in the district. They have been dated at 5.9±0.2 m.y. by the K-Ar method (Albers and Stewart, 1972; Robinson and others, 1968). Some of the porphyritic rhyolite appears as isolated areas on the geologic map of the district (pl. 1), but the visible spatial and stratigraphic relations and the mineralogy make it obvious that these areas are directly related.

A small volcanic butte (fig. 7) located 1.8 km east of the Nivloc mine (pl. 1) was probably the vent for this rock. Attitudes of the flow banding range from almost horizontal at the base to nearly vertical at the center. Where exposed, the basal section is quite frothy and glassy and has baked the underlying material. This vent is physically connected with some of the porphyritic rhyolite flows and may have been connected with all of them before the erosional breaks occurred.

The porphyritic rhyolite is gray to red gray with abundant phenocrysts set in a holohyaline groundmass. Phenocrysts are exceptionally well formed and consist of quartz, plagioclase, sanidine, hornblende, biotite, and sphene. Quartz phenocrysts, which are generally subhedral, are usually deeply embayed, and a few are biaxial

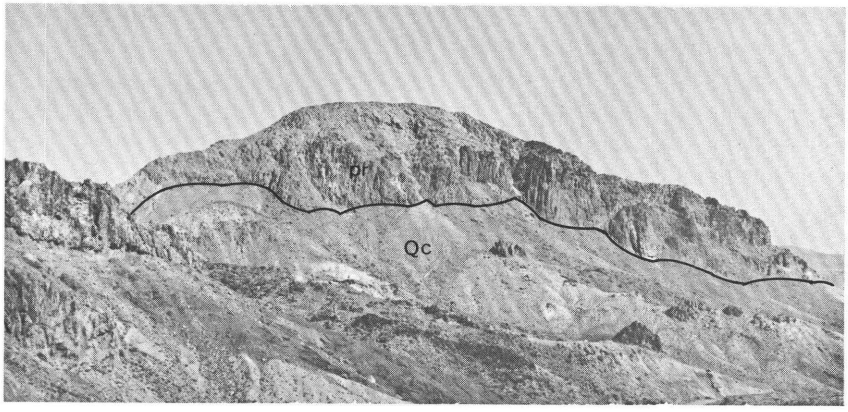

FIGURE 7.—Butte-shaped vent for one of the porphyritic rhyolite flows (pr). *Qc*, colluvium.

($2V$ =3–4°). They are usually large enough (up to 2.5 mm) for the embayments to be seen in hand specimens. The plagioclase phenocrysts are oligoclase-andesine (An_{18-35}) and are generally 2–4 mm long. Some of the plagioclase phenocrysts occur in clots that are either monomineralic or contain plagioclase, hornblende, and sporadic sanidine and biotite. The plagioclase phenocrysts are usually complexly twinned with albite, Carlsbad, and possible pericline twinning. The sanidine occurs as euhedral to subhedral crystals up to 4 mm long and also forms rims around the plagioclase phenocrysts. Many of the phenocrysts exhibit fresh fracturing, but this may be a function of thin section manufacture. The hornblende is generally unaltered, usually twinned, euhedral to subhedral, and as much as 2 mm long. The phenocrysts are pleochroic from yellow brown to yellow green. The biotite is red brown and generally fresh, although some phenocrysts have red oxidation rims. Sphene occurs as yellow-brown euhedral crystals up to 1 mm long. The apatite and zircon crystals together make up less than 1 percent of the total rock; zircon is much less abundant than apatite.

The normative anorthite composition of the porphyritic rhyolite as represented by sample 482 (An_{21}) (table 1) falls within the range of phenocryst composition (An_{21-35}) (samples 2, 4, and 482, table 2). The modal composition of this rock indicates minor K-feldspar (7 percent, table 2), but the chemical analysis shows 5.6 percent K_2O and 33.9 percent normative orthoclase (table 1). Staining of these rocks indicates that much of the K_2O is present in the glassy groundmass. These rocks are also high in SiO_2, which is reflected by the high (29 percent) normative quartz (table 1).

PORPHYRITIC RHYOLITE DIKE

A porphyritic rhyolite dike trends approximately N.40°E. across the west-central part of the district (pl. 1). The dike provides the evidence for the stratigraphic relations between the porphyritic rhyolite, latite, and mineralization in the district. This rock was formed contemporaneously with the porphyritic rhyolite flows and is therefore one of the youngest volcanic units in the district. The dike tends to form cliffs that average about 4 m in height. The north end of the dike has widened and formed a sill-like body that has vertical columnar jointing.

The porphyritic rhyolite dike is older than the mineralizing fluids and has been hydrothermally altered by them, although the degree of alteration varies from outcrop to outcrop. The degree of alteration appears to be greater in the vicinity of the surface exposure of the Sixteen-To-One vein. The alteration is mainly sericitic. Finely disseminated pyrite occurs sporadically throughout the dike.

The dike is mineralogically similar to the porphyritic rhyolite flows. It contains phenocrysts of quartz, plagioclase, sanidine, hornblende, biotite, sphene, and small amounts of apatite and zircon. These are set in a cryptofelsitic groundmass that consists almost exclusively of K-feldspar. Quartz phenocrysts in this rock are deeply embayed and commonly form micrographic textures with K-feldspar. Plagioclase, which ranges from oligoclase to andesine (An_{23-35}), generally exhibits slight oscillatory zoning as well as complex twinning. It occurs as large (up to 4 mm) euhedral to subhedral crystals, both as single crystals and in polymineralic glomeroporphyritic clots. Sanidine is less abundant in this rock than in the porphyritic rhyolitic flows (table 2). It occurs as discrete crystals as well as rims completely enclosing some plagioclase phenocrysts. Hornblende is almost entirely replaced by biotite, but relics still display subhedral outlines as much as 1.4 mm in diameter.

Biotite and sphene are nearly the same in both the porphyritic rhyolitic flows and dike. Biotite occurs as thin red-brown laths, and sphene as small (<0.6 mm) euhedral crystals.

Accessory apatite and zircon are similar to those found in the porphyritic rhyolite flows. They occur as inclusions in the phenocrysts and constitute less than 1 percent of the rock. The apatite inclusions are unusually long (up to 0.25 mm).

Chemical analyses for this rock (samples 279 and 479, table 1) show a slight decrease in CaO and a slight increase in Na_2O and K_2O relative to the porphyritic rhyolite flows, but those differences are insignificant. Because the rock is entirely altered, the alteration must have come mainly from a remobilization of the existing elements by the hydrothermal fluids.

ROCK CHEMISTRY

The volcanic rocks in the Red Mountain mining district form a calcic-rich alkali-calcic suite ranging in composition from andesitic to rhyolitic using the classification of Rittmann (1952) (fig. 8) or basaltic to rhyolitic by the classification of Taylor (1969) (fig. 9). The alkali-lime index is 55.6, which places the suite in the alkalic-calcic grouping of Peacock (1931). The index was determined assuming linear relations between total alkalis and silica, and lime and silica, and calculating a regression line for each.

Chemical analyses of the igneous rocks in the Red Mountain district (table 1) are representative of the entire Silver Peak volcanic center. This is evident when the analyses of the district rocks are compared with those of the rest of the Silver Peak volcanic center (Robinson, 1972). The analyses presented by Robinson (table 1) include rocks from the rest of the volcanic center and form the same

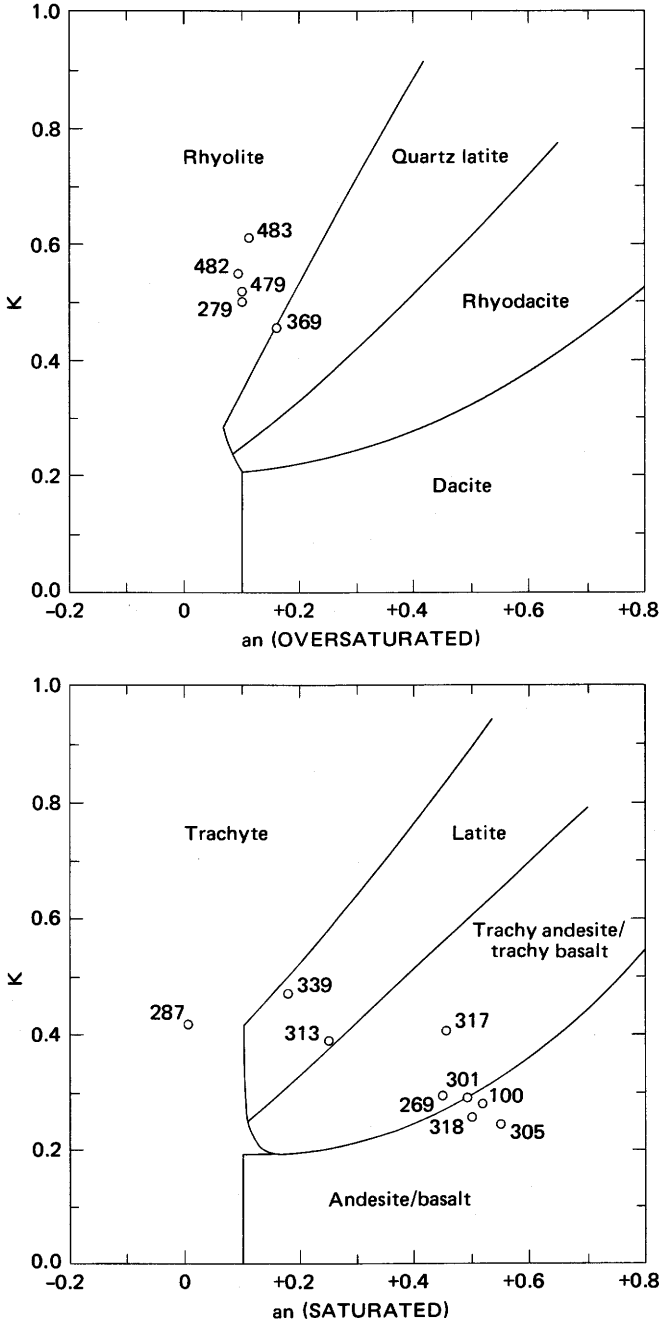

FIGURE 8.—Classification of the volcanic rocks in the Red Mountain mining district by the Rittmann chemical method (modified from Rittmann, 1952). The an and K values are calculated from weight percent as follows:

$$an = (0.9\ Al_2O_3 - K_2O - 1.5\ Na_2O)/(0.9Al_2O_3 + K_2O + 1.5\ Na_2O)$$
$$K = (K_2O)/(K_2O + 1.5\ Na_2O)$$

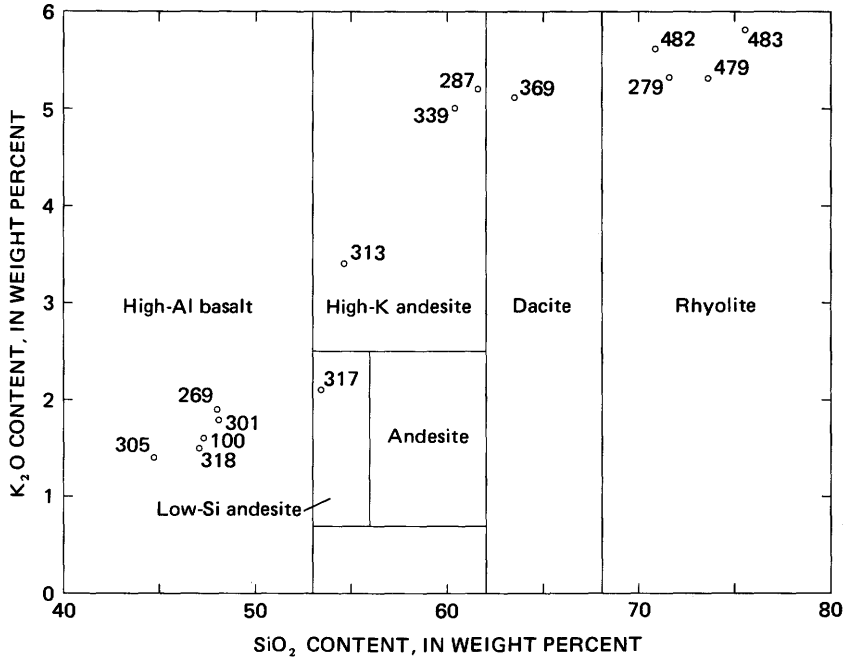

FIGURE 9.—Classification of the volcanic rocks in the Red Mountain mining district by the Taylor method (modified from Taylor, 1969).

general trends as those from the Red Mountain district, as represented by the silica variation diagrams of figure 10.

With the exception of magnesia and alumina, the silica variation diagrams (fig. 10) show the smooth trends one would expect if the rocks were genetically related and were derived from a differentiation process (Krauskopf, 1967, p. 399). The variation diagrams for magnesia and alumina apparently each show two trends. One of these in each diagram is normal in that it shows gradually decreasing weight percent of magnesia and alumina accompanying an increase in silica. On the alumina diagram, the other trend shows a sharp decrease in the weight percent of the alumina with an increase in the weight percent of silica and, on the magnesia diagram, a sharp increase in magnesia with an increase in the weight percent of silica. These abnormal "trends," which are confined to the basaltic rocks, are due simply to scatter apparently resulting from the accumulation of varying amounts of both mafic minerals and feldspar crystals in these rocks. The scatter in figure 10 is generally greater in the more basic rocks as one would expect, because the more basic rocks contain a larger percentage of phenocrysts and would, therefore, deviate more from the magma composition. The arrows in figure 10 connect the major oxide analyses for sample 305 (table 1) to the oxide analyses with the phenocryst composition and quantity removed (x) (table 2).

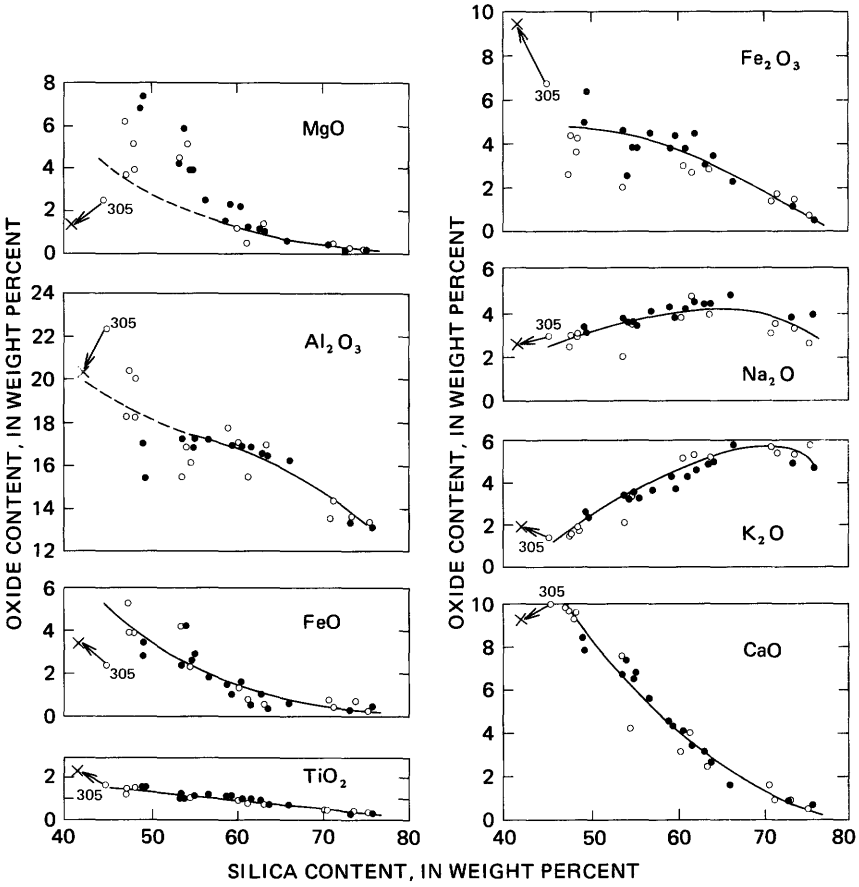

FIGURE 10.—SiO_2 variation diagrams of common oxides of the volcanic rocks of the Silver Peak volcanic center. Circles represent analyses from this study, and dots represent analyses from Robinson (1972).

This approximates the theoretical composition of the melt at the time of solidification.

The alkalic nature of the Silver Peak volcanic suite illustrated by the Peacock index can also be seen in the F'MA and K_2O–CaO–Na_2O ternary diagrams (fig. 11). The F'MA diagram shows a smooth trend of increasing alkalis and a relative decrease in FeO and MgO. The K_2O–CaO–Na_2O diagram shows a similar increasing trend with a decrease in lime. These diagrams also illustrate the relation between the alkali-calcic Silver Peak volcanic suite and the general trends of calc-alkalic suites (Best, 1969). The more mafic rocks of the Silver Peak suite contain more alkalis and magnesium relative to iron than those rocks of calc-alkalic composition and, in general, more potassium and lime relative to sodium.

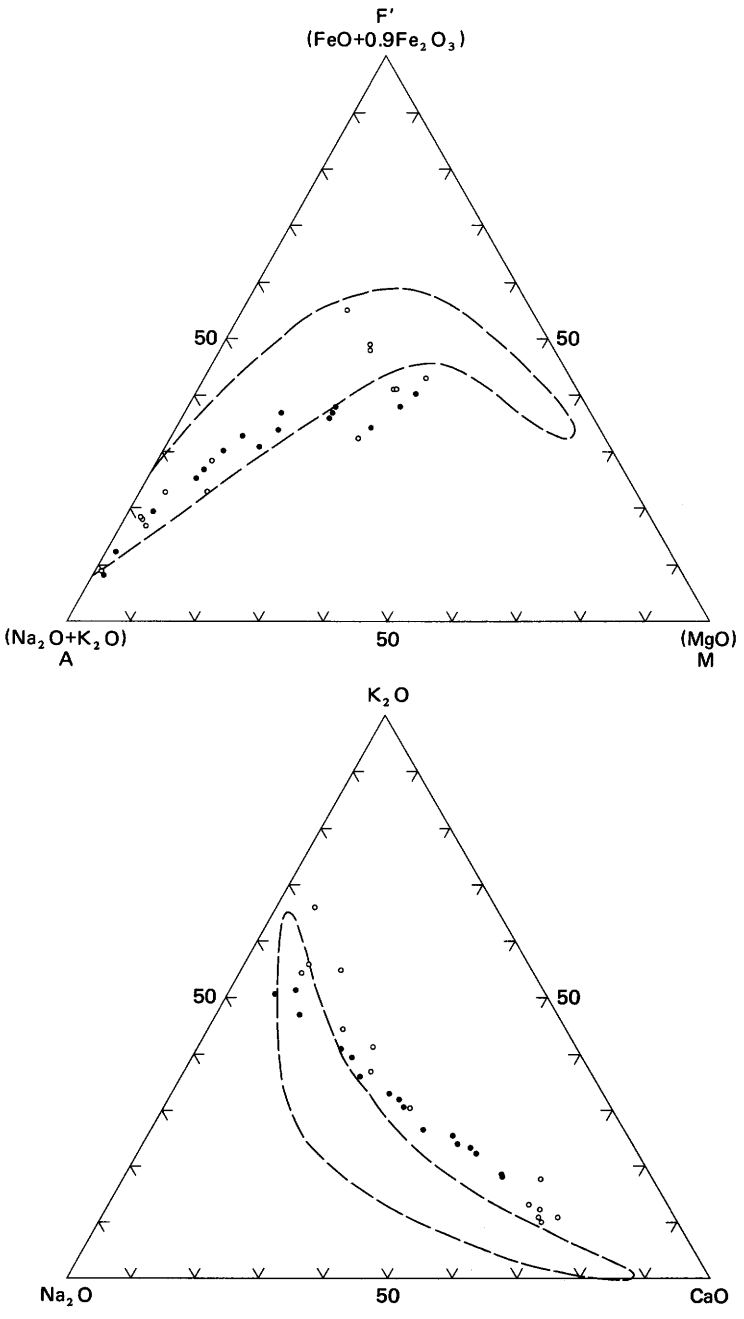

FIGURE 11.—F'MA and K_2O–CaO–Na_2O ternary diagrams for representative volcanic rocks of the Silver Peak volcanic center. Circles, analyses from this study; dots, analyses from Robinson (1972); dashed envelope, region of normal calc-alkalic rock suite (modified from Best, 1969).

The CIPW normative mineral percentages for the Silver Peak volcanic center analyses are listed in table 1. These percentages show a steady increase in the alkali concentration in the rocks as the differentiation process continued and produced more silica-rich rocks. The ternary diagram for the normative feldspars (fig. 12) illustrates this point and also the high initial concentration of lime in the Silver Peak volcanic suite.

All the variation diagrams discussed so far, except those for MgO and Al_2O_3, have exhibited smooth trends and relatively small scatter envelopes. These smooth trends have been interpreted as an indication that the rocks are probably related in origin and are part of a differentiated rock suite (Bowen, 1956; Nockolds and Allen, 1953; Turner and Verhoogen, 1960, p. 77).

The chemical analyses and petrography of these rocks indicate magmatic differentiation of the original magma involving fractional crystallization on the basis of the following:

1. Some of the plagioclase phenocrysts in the andesites exhibit synneusis textures (fig. 2) similar to those described by Vance (1969); thus the phenocrysts were probably formed in the parental magma rather than entering the magma as xenocrysts.
2. The phenocrysts and glomeroporphyritic clots are monomineralic, except for small inclusions of other minerals. If these phenocrysts were derived from another source, then they would probably be polymineralic. Vance and Gilreath (1967) demonstrated that monomineralic glomeroporphyritic clots are also a product of synneusis.
3. The phenocrysts, including labradorite, olivine, and augite, are minerals that crystallize early in an andesitic magma.

More evidence supporting the crystal fractionation hypothesis can be found in the silica variation diagrams for the minor elements (fig. 13). Crystal fractionation would be expected to deplete the magma of iron, magnesium, titanium, manganese, calcium, copper, cobalt, nickel, scandium, chromium, and vanadium and concentrate potassium, sodium, zirconium, lead, and lanthanum with the extrusion of the more mafic rocks. These conditions and also the trends that formed as composition of the magma changed from basic to more silicic, are shown in figures 10 and 13.

The silica variation diagram for strontium indicates that the magma was steadily depleted in strontium until there was virtually none left. Strontium probably was tied up in the plagioclase formed in the more basic rocks.

Six samples from this study (318, 313, 339, 369, 482, 483) were also analyzed for palladium, platinum, and rhodium by the method of Haffty and Riley (1968), but these elements were all below the limit of detectability.

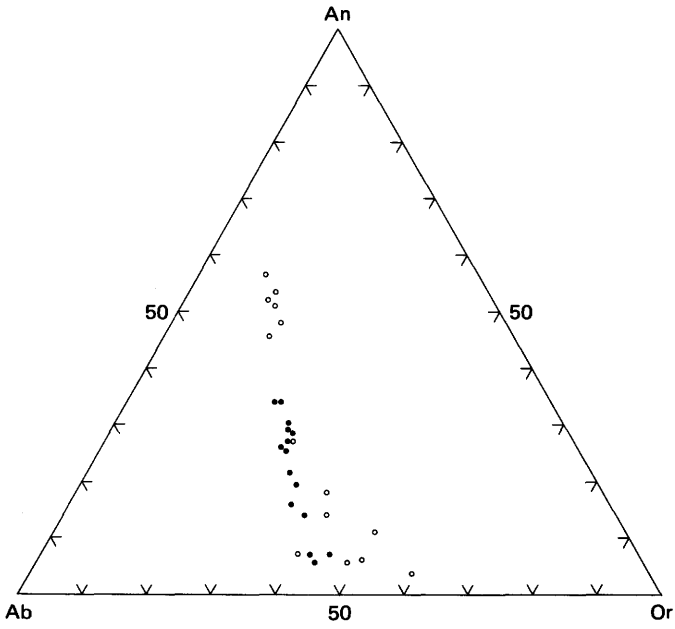

FIGURE 12.—Normative An-Or-Ab ternary diagram for representative volcanic rocks of the Silver Peak volcanic center. Circles, analyses from this study; dots, analyses from Robinson (1972).

STRUCTURE

Faults in the Red Mountain mining district generally strike about N. 20–40°E., although the Basin and Range trend here is northerly (Albers, 1967). Therefore some model other than Basin and Range deformation must by developed to explain the northeasterly orientation. The structure in the district can be clarified by considering a larger area (fig. 14). The Red Mountain mining district is part of a rectangular-shaped structural block (fig. 14) bounded on the northeast by Precambrian and Paleozoic sedimentary rocks, which are intruded by the Mineral Ridge pluton of Mesozoic age, and on the southwest by Paleozoic sedimentary rocks, which are intruded by the Palmetto pluton of Jurassic age (Albers and Stewart, 1972).

This structural block, herein called the Silver Peak block, lies within a belt of right-lateral deformation near the west edge of the Basin and Range province. The major structural features are the Silver Peak–Palmetto–Montezuma oroflex of Albers (1967), the Walker Lane (Billingsley and Locke, 1939; Locke and others, 1940), and the Death Valley–Furnace Creek fault zone of Curry (1938). A fourth feature of the Silver Peak block, not related to the right-lateral

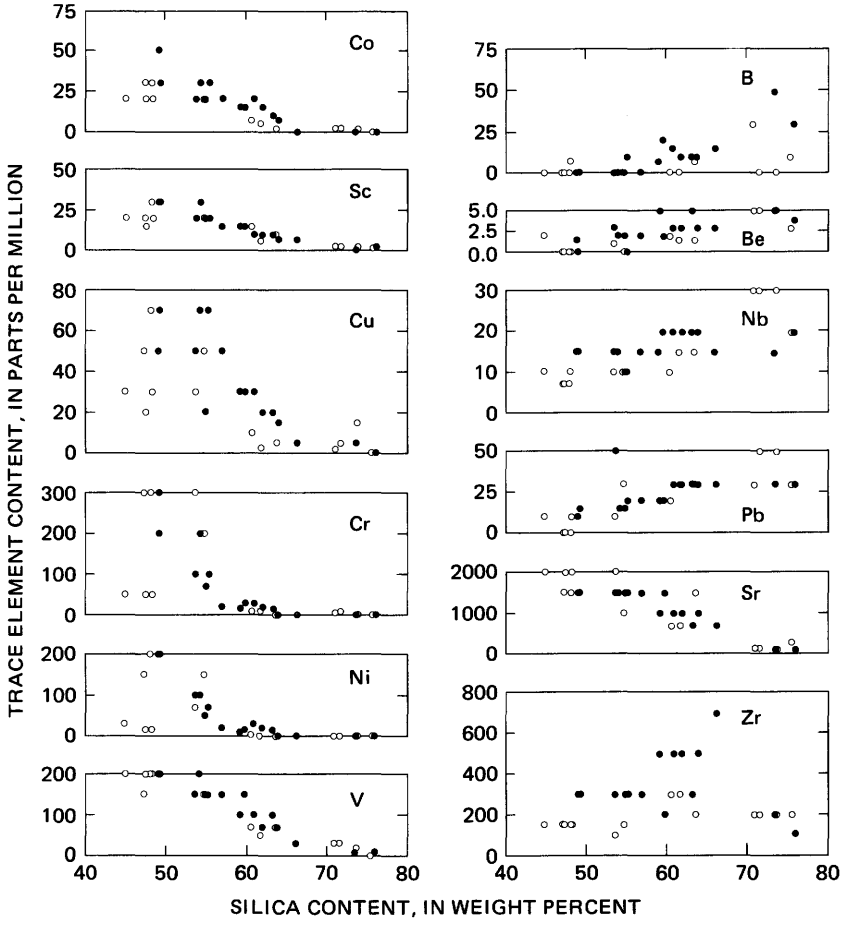

FIGURE 13.—SiO_2 variation diagrams for selected trace elements in representative rocks from the Silver Peak volcanic center. Circles, analyses from this study; dots, analyses from Robinson (1972).

deformation, is the Silver Peak collapse caldera of Robinson (1968).

Albers (1967) delineated a series of large-scale nested sigmoidal structural trends in the area on the basis of the arcuate trends of mountain ranges and Paleozoic carbonate facies boundaries. He used the term "oroflex" to describe these features, defining it as "a mountain range with an arcuate trend that is believed to have been inherited from tectonic bending of the crust" (Albers, 1967, p. 145).

The Silver Peak block forms a part of the Silver Peak–Palmetto–Montezuma oroflex. Oroclinal flexuring in the rocks between the Death Valley–Furnace Creek fault zone and the Walker Lane was

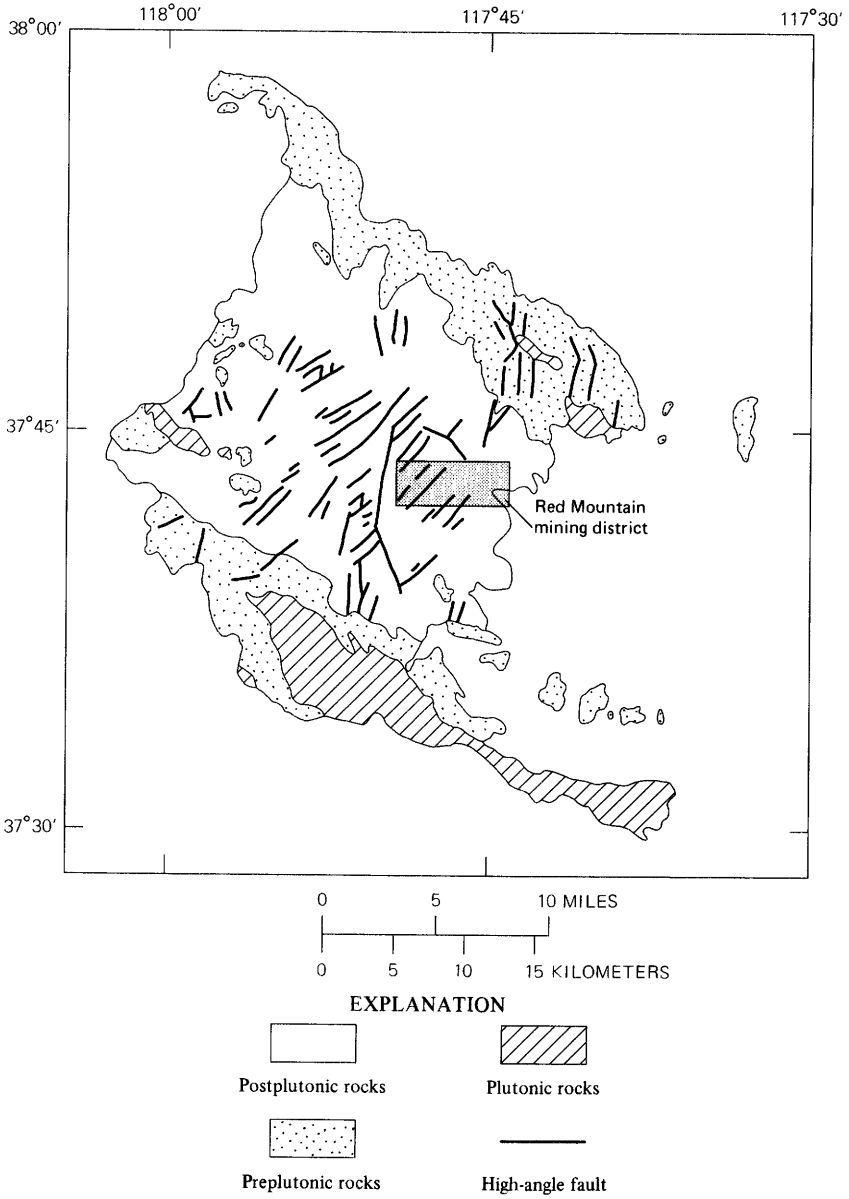

FIGURE 14.—Generalized geologic and structure map of the Silver Peak structural block after Albers (1967) and Albers and Stewart (1972).

proposed as the initial deformation forming in response to the build-up of stress in the block (Stewart, 1967; Albers, 1967). Albers(1967, p. 153) concluded that the bending in the area was concluded by early to middle Miocene and that the movement since that time has been

limited to right-lateral faulting. The Silver Peak block forms the northwest-trending west limb of the oroflex, and the basement trend thus does not control the northeast structural trend seen in the volcanic rocks.

The Walker Lane, located about 50 km northeast of the Silver Peak block (fig. 15), is a northwest-trending lineament that is characterized by right-lateral offsets. It marks the northeast limit of a belt of chaotic topography near the west edge of the Basin and Range physiographic province of Fenneman (1931). This belt includes the "whorls and loops" of Locke, Billingsley, and Mayo (1940). Albers (1967, p. 151) indicated that right-lateral deformation in this area began as early as middle or late Early Jurassic. This type of deformation is still occurring as evidenced by historic right-lateral movement on faults recorded in this area (Gianella and Callaghan, 1934). Several miles of right-lateral displacement have been proposed for the Walker Lane by Ferguson and Muller (1949, p. 14), Longwell (1960, p. 197), and Shawe (1965, p. 1361).

The general trend of faults in the Silver Peak block is N. 20°E. to N. 40°E., which is nearly perpendicular to the trend of the Walker Lane. The northeast structural trend in the block is proper for faults developing as synorogenic complements to major right-lateral displacement along the Walker Lane. However, for these to be true complementary structures, the offsets should be left lateral, but evidence of any left-lateral movement on these faults is lacking. The faults are high-angle normal faults that formed in response to crustal extension. However, tensional faults related to north-south crustal shortening should trend due north. The only faults in the area that meet the requirements for tensional faults related to the Walker Lane are the younger, north-trending Basin and Range faults, which Shawe (1965) theorizes could be expected to occur in areas of right-lateral deformation. Thus, the forces that produced the Walker Lane were probably not directly responsible for the northeast-trending faults in the Red Mountain mining district.

The Death Valley–Furnace Creek fault zone (fig. 15) is a northwest-trending right-lateral strike-slip fault zone. The zone parallels the California-Nevada State line in the vicinity of Esmeralda and Nye Counties, Nev., and marks the southwestern boundary of the chaotic topographic belt. The northern limit of Death Valley–Furnace Creek fault zone is located in the north end of Fish Lake Valley (Albers, 1967). McKee (1968) believes, on the basis of a potassium-argon isotopic age on sediments found in the south end of the Fish Lake Valley graben, that the fault zone is at least late Miocene in age and possibly older. Various authors disagree on the amount of horizontal offset but agree on the direction of movement. Estimates of displacement range from a few kilometers at most

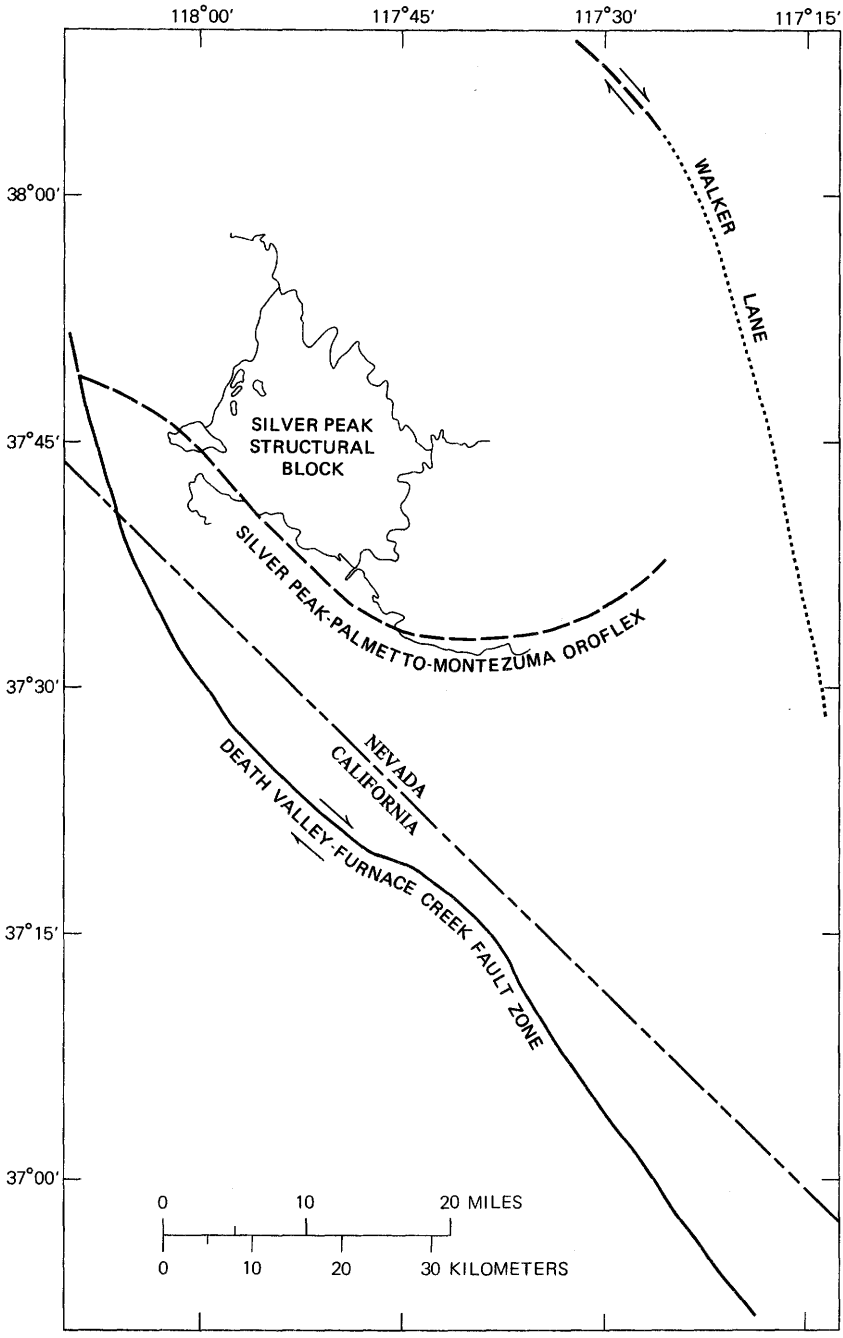

FIGURE 15.—Location of the Silver Peak structural block in relation to the Death Valley–Furnace Creek fault zone, the Silver Peak–Palmetto–Montezuma oroflex, and the Walker Lane.

(Wright and Troxel, 1966) to 80 km (Stewart, 1967). Recent movement along the fault zone has been demonstrated by Curry (1938).

The major structures in the block trend nearly perpendicular to the Death Valley–Furnace Creek fault zone, as they do to the Walker Lane. By analogy to the Walker Lane, the faults in the Silver Peak block are apparently not related to the deformation that produced the Death Valley–Furnace Creek fault zone.

The central part of the Silver Peak Range is a volcanic center (Albers and Kleinhampl, 1970; Albers and Stewart, 1972; Robinson, 1968, 1972; Robinson and others, 1968). Robinson (1972, 1968) and Robinson, McKee, and Moiola (1968) proposed that a collapse caldera exists in the central Silver Peak area. The faults in the Red Mountain mining district could be considered part of a ring fracture system associated with the larger structure. However, high-angle, northeast-trending normal faults are predominant in the entire Silver Peak block, and there is no compelling reason to think that some of them are part of a ring fracture system. Where the faults cross the proposed boundaries of the caldera, they do not change in trend or direction of displacement.

Robinson (1972, p. 1692) estimated that 4 km^3 of lava was erupted from the volcanic center in a 1–1.5-m.y. period. The probability is strong that subsidence occurred in the area during and after the eruption of the lavas. Preexisting structures having a northeast trend could be responsible for the northeast trend of faults that accompanied subsidence. However, preexisting structures need not be called upon to explain the northeast-trending faults. The faults could be, and probably were, produced by subsidence accompanied by a northwest-southeast crustal extension of the Silver Peak block.

MINERAL DEPOSITS

VEINS

In the Red Mountain mining district, sheeted quartz-calcite fissure veins bear silver and minor amounts of gold, lead, zinc, and copper. Most of the veins occur in northeast-trending fault zones. The major ore mineral in the district is argentite (acanthite)[1] (Albers and Stewart, 1972, p. 71; Albers and Kleinhampl, 1970, p. C6). The gangue minerals other than quartz and calcite are barite, siderite, and possibly manganosiderite. Nearly all of the veins carry some manganese minerals, and some, such as the Mohawk, carry large

[1]Argentite reverts to acanthite when the temperature drops below approximately 173°C (Boyle, 1968, p. 19; Frueh, 1958, p. 137; Ramsdell, 1943, p. 401).

amounts. Hewett and Radtke (1967) have shown that at least some of the manganese oxides in the Mohawk mine are hypogene.

The host rocks for the veins are the layered volcanic and sedimentary rocks in the district (see pl. 1). Some of the veins (Mohawk and Sixteen-To-One) crosscut the latite, which is approximately 6 m.y. old, making the deposits latest Miocene or early Pliocene in age.

The major controlling factors in the mineralization of the district are the faulting and fracturing that existed at the time the mineralizing fluids were active. Fractured areas caused by faulting created channels for the mineralizing fluids. These channels plus replacement processes and the mineralizing fluids have formed the veins in the Red Mountain mining district.

The veins in the district are all steeply dipping epithermal fissure veins. Their depth from the surface at the time of emplacement was probably about 200 m, assuming an erosion rate of 0.3 m per 9,000 years (Gilluly and others, 1959, p. 71). This rate is based on the sediment loads carried by present-day streams and probably represents a maximum. Using 200 m as a maximum depth of cover, the curves of Haas (1971) indicate the maximum temperature to be 210°C. This temperature estimate is supported by heating-stage studies of fluid inclusions in one sample of vein quartz which indicate that the fluids that deposited the veins were boiling (J. T. Nash, oral commun., 1972).

At the surface, the veins consist of friable masses of quartz seldom exceeding 1.8 m in width that have been leached of carbonate, sulfides, clays, and most of their silver. Locally boxworks and vugs containing quartz crystals persist, but at most localities such features were destroyed because the highly porous skeletal mass of quartz has collapsed between the massive volcanic rocks that form the vein walls. The leaching of vein material and collapse of vein walls near the surface results in a marked decrease in vein widths. The Sixteen-To-One vein has an average surface width of about 1.8 m and an average width of 15 m at a depth of 90 m.

ALTERATION

Although almost all of the rocks of the district are altered to some degree, distinct zonal relations around veins were not observed. Many of the rocks in the district display weak to moderate propylitic alteration and have an overprint of silicification or argillization. The silicification is usually associated with the intrusive rhyolite and tends to form halos of silicified rock around the rhyolitic intrusive rocks.

The veins, associated faults, and the wallrocks of the veins and faults are argillized and silicified. Argillization is more extensive

than silicification, and the argillized rocks are generally bleached white, but some are orange or red. The altered areas shown on plate 1 represent both silicified and argillized rock.

ECONOMIC GEOLOGY

HISTORY

The Red Mountain mining district was opened in 1907 with the discovery of the Nivloc mine (Albers and Stewart, 1972). Since that time it has produced more than 4 million ounces of silver, 18,000 ounces of gold, 24,000 pounds of lead, 8,000 pounds of zinc, and 700 pounds of copper (U.S. Bur. Mines, unpub. data). The two major producers in the district are the Mohawk (Argentite) mine (see pl. 1) on the west end of the district and the Nivloc mine (pl. 1) on the east end. The Sixteen-To-One vein was discovered around 1920 at approximately the same time that the Mohawk mine opened (Albers and Stewart, 1972, p. 71) and is located approximately halfway between the Nivloc and Mohawk mines. The Sixteen-To-One mine, at the time of the author's field mapping, was being developed but was not yet in production.

ORE DEPOSITS

The Red Mountain mining district includes four mines with production records: Mohawk, Nivloc, Sanger, and Coyote; one that is reported to be nearing production is the Sixteen-To-One. The Coyote and Sanger mines, which are outside of the map area, were minor producers, whereas the Nivloc and Mohawk mines were major ones.

The Mohawk (Argentite) mine is located in the NE¼ sec. 36, T. 25 S., R. 37 E. (unsurveyed) (fig. 1). Although it was first operated around 1920, its major production was from 1952–1958. Production included silver and gold and minor amounts of lead, zinc, and copper. Albers and Stewart (1972, p. 71) reported that the ore averaged about 20 to 25 ounces of silver per ton. The mine was developed to a depth of more than 183 m. Oxidation extended to the bottom of the mine.

The Mohawk vein contains the largest amount of manganese of any of the veins in the district. Hewett and Radtke (1967) analyzed a number of silver-bearing black calcite samples from various mining districts in the Western United States and ascertained whether the manganese oxides are hypogene or supergene. A sample from the Mohawk mine contained manganese oxides that were clearly hypogene. This raises the possibility that the smaller amounts of manganese oxides in other veins in the district are also hypogene in origin.

The Nivloc mine is located in the SE¼SE¼ sec. 33, T. 25 S., R. 38 E. (fig. 1) and at one time supported the now-abandoned town of Nivloc. The mine had its chief production during the period 1937–43 when it

produced ore worth $2 to $3 million. The ore mined during this period averaged about 11 ounces per ton of silver and 0.05 ounces per ton of gold (Albers and Stewart, 1972, p. 71).

The Nivloc mine reached a depth of 396 m down dip and consisted of a zone of veins as wide as 24 m at an approximate depth of 91 m. The base of the Tertiary section is penetrated at this depth, and the veins shrink in width as they pass through this boundary; the veins are 9 m wide on the 900 level of the mine (A. Baker, 3d, unpub. geol. rept.).

Claims were staked on the Sixteen-To-One property in the 1920's and 1930's. Although there has been no recorded production, the mine has been explored by several companies. Exploration consists of more than 3,300 feet of access tunnel, drifts, and crosscuts on a single level, and a few raises (fig. 16). The vein has been explored below this level by several inclined boreholes.

The Sixteen-To-One vein, like the other veins in the district, is a steeply dipping epithermal fissure vein. It trends approximately N. 55° E. and dips overall about 75° SE., but individual attitudes taken on the surface show dips ranging from 75° N. to 80° S. Outcrops of the vein, which may reach 3 m in width but average about 1.5 m, consist of friable quartz and minor calcite. Vein widths in the exploration crosscuts approximately 122 m below the surface reach at least 10.7 m. Core drill data indicate that the vein persists to a depth of at least 253 m where the width is approximately 12 m (A. Baker, 3d, unpub. geol. rept.).

The vein, where exposed in the exploration workings, is composed mostly of quartz and calcite and minor galena, sphalerite, chalcopyrite, acanthite, and clay minerals. All the ore minerals were identified microscopically; galena and sphalerite were confirmed by X-ray diffraction. The vein is divided into two sections. The hanging wall side is composed largely of sheeted quartz-calcite and pockets of manganese oxides and clay. Much of the sheeted quartz-calcite includes black calcite similar to that described by Hewett and Radtke (1967) in the Mohawk mine. Although sulfide minerals are scarce, they usually occur in this sheeted section rather than the footwall section. Figure 17 shows the sharp contacts and some of the sheeting between the vein and wallrock in the hanging wall area. The footwall side of the vein at most places is composed almost entirely of massive calcite partially or completely replaced by quartz. Quartz pseudomorphs after calcite commonly occur in this section.

A series of geochemical samples taken in the Sixteen-To-One mine from the portal, across the Sixteen-To-One vein, to the wallrock on the north side of the vein were chemically analyzed (Ashley and Keith, 1971). Figure 18 illustrates the trends of selected elements

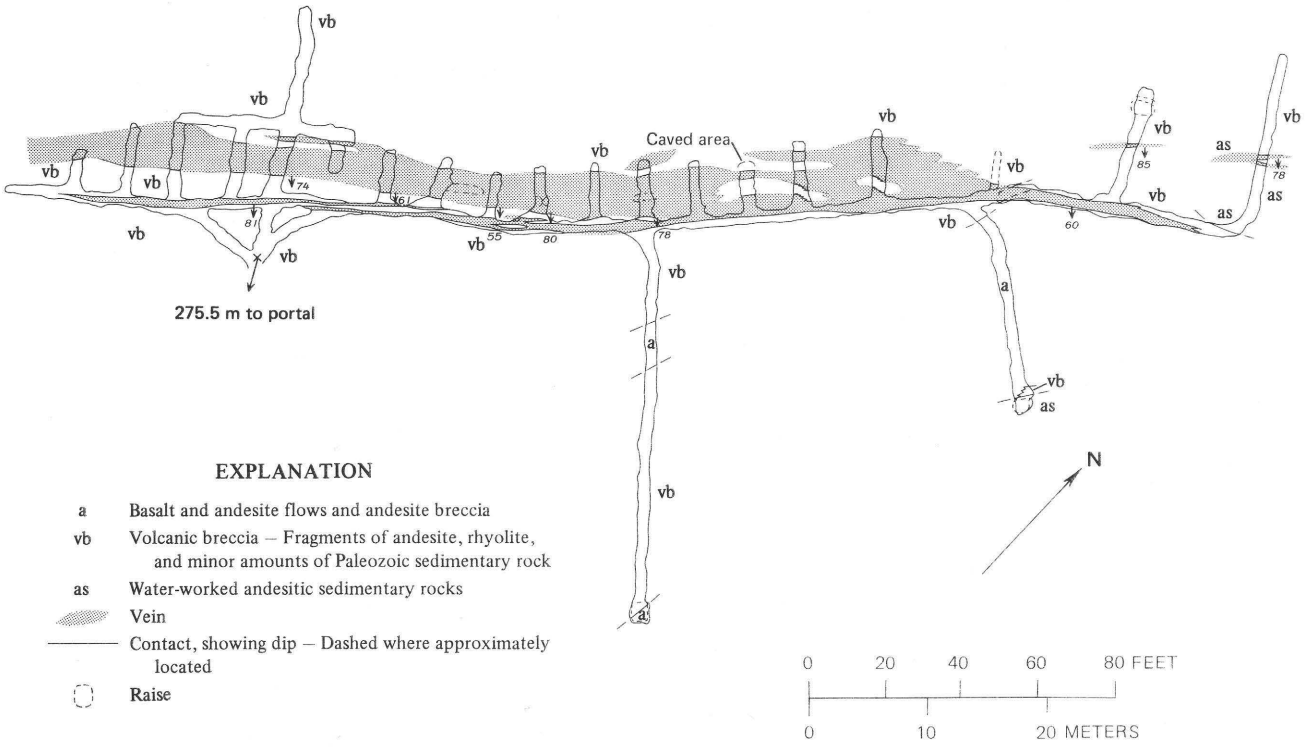

FIGURE 16.—Generalized geologic map of the Sixteen-To-One mine.

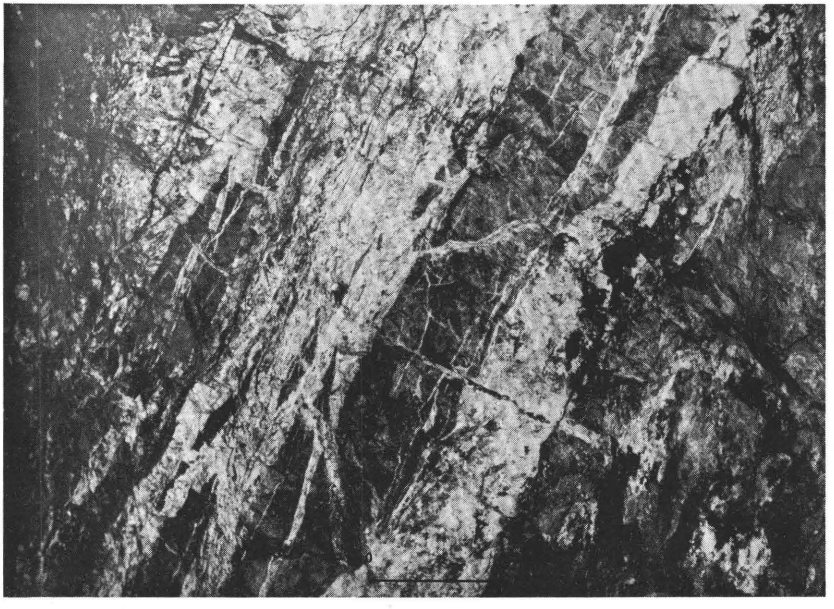

FIGURE 17.—Sheeting in vein and sharp boundaries between vein material and wall-rock in the Sixteen-To-One mine, Esmeralda County, Nev.

proceeding from unaltered rock to silica veins as calculated from the chemical data. The expanding envelopes in the figure display the tendency for the selected elements to increase in variability or inhomogeneity from relatively fresh rock into carbonate and silica veins. Keeping in mind that much, if not all, of the silica emplacement was subsequent to carbonate deposition, the means for silver, gold, lead, and beryllium may indicate the preference of these elements for either silica or carbonate veins or they may simply represent more than one period of deposition. Silver, gold, and beryllium increase in the silica veins relative to the carbonate veins, and lead is more concentrated in the carbonate veins (fig. 18). Although the mean value for arsenic remains nearly the same through the host rock and the veins, the variability increases dramatically in the silica veins. The zinc diagram is cut off at both ends because the values, if any, were below the detectable limits of the analytical method used in the unaltered rock and the silica veins. These elements tend to decrease in quantity as well as variability in the silicified rocks.

The Coyote and Sanger mines, which lie north of the mapped area, have the same general geology as the Nivloc, Mohawk, and Sixteen-To-One mines and similar northeast-trending steeply dipping fissure veins. Both mines have produced silver, and although the Coyote was

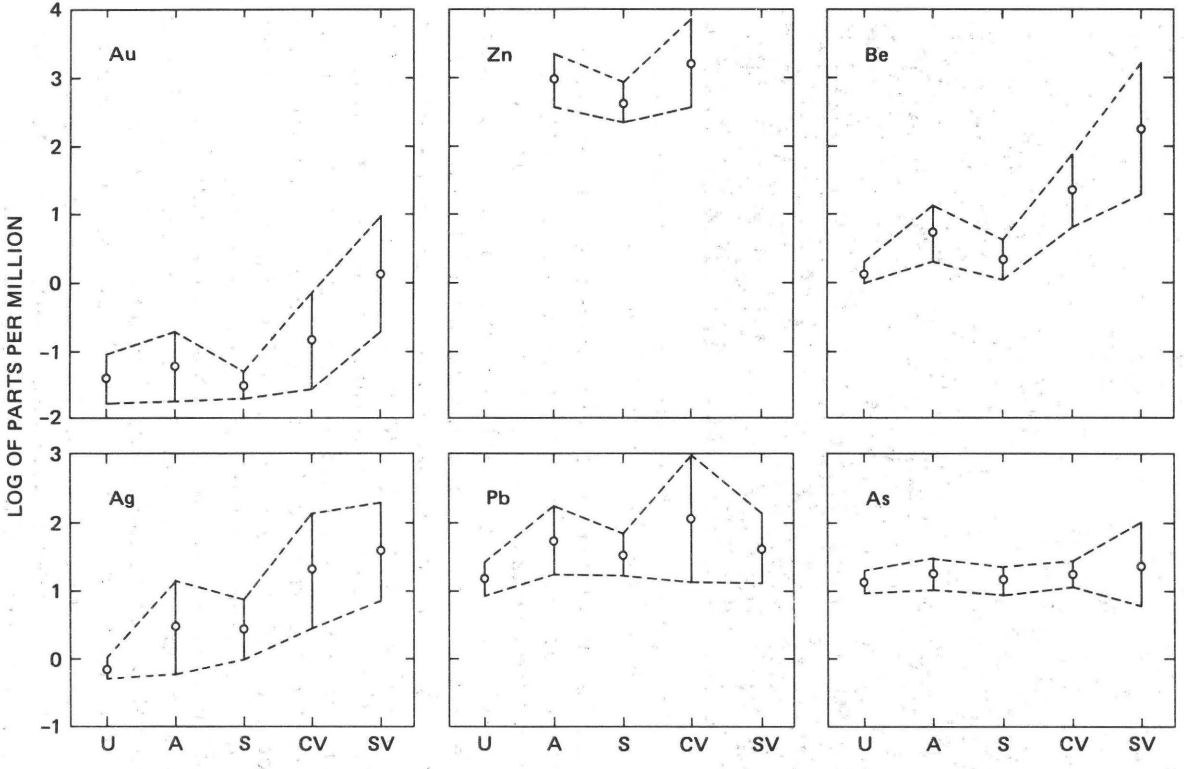

FIGURE 18.—Graph showing relation between log ppm of silver, gold, lead, zinc, arsenic, and beryllium in unaltered rocks (U), argillized rock (A), silicified rock (S), carbonate veins (CV), and silica veins (SV) in the Sixteen-To-One mine. Circles represent geometric mean of the log ppm of the element. Dashed envelope represents one standard deviation above and below the mean.

not in operation at the time of the field mapping, the Sanger is still producing.

A few minor prospect pits and short adits occur in the district, mostly on the northeast-trending veins. Some have been explored by diamond drilling.

REFERENCES CITED

Albers, J. P., 1967, Belt of sigmoidal bending and right-lateral faulting in the western Great Basin: Geol. Soc. America Bull., v. 78, p. 143–156.

Albers, J. P., and Kleinhampl, F. J., 1970, Spatial relation of mineral deposits to Tertiary volcanic centers in Nevada, *in* Geological Survey research 1970: U.S. Geol. Survey Prof. Paper 700–C, p. C1–C10.

Albers, J. P., and Stewart, J. H., 1972, Geology and mineral deposits of Esmeralda County, Nevada: Nevada Bur. Mines Bull. 78, 80 p.

Ashley, R. P., and Keith, W. J., 1971, Geochemical data for the Sixteen-To-One mine, near Silver Peak, Esmeralda County, Nevada: U. S. Geol. Survey open-file report, 30 p.

Bailly, P. A., 1951, Geology of the southeastern part of Mineral Ridge, Esmeralda County, Nevada: Stanford Univ., Stanford, Calif., Ph. D. thesis; 1953, abstract in Stanford Univ. Abs. Dissert. 1951–52, v. 27, p. 415–417.

Best, M. G., 1969, Differentiation of calc-alkaline magmas, *in* Andesite Conf., Eugene and Bend, Oreg., 1968, Proc. (Internat. Upper Mantle Prof. Sci. Rept. 16): Oregon Dept. Geology and Mineral Industries Bull. 56, p. 65–75.

Billingsley, P. R., and Locke, Augustus, 1939, Structure of ore districts in the continental framework: New York, Am. Inst. Mining Metall. Engineers, 55 p.

Bowen, N. L., 1956, The evolution of the igneous rocks: New York, Dover Publishers, Inc., 332 p.

Bowen, R. W., 1972, Graphic normative analysis program: Natl. Tech. Inf. Service, NTIS Rept. PB2–06736, 85 p.

Boyle, R. W., 1968, The geochemistry of silver and its deposits, with notes on geochemical prospecting for the element: Canada Geol. Survey Bull. 160, 264 p.

Curry, H. D., 1938, Strike-slip faulting in Death Valley, California abs.: Geol. Soc. America Bull., v. 49, p. 1874–1875.

Curtis, G. H., 1954, Mode of origin of pyroclastic debris in the Mehrten Formation of the Sierra Nevada: California Univ. Pubs. Geol. Sci., v. 29, p. 453–502.

Durrell, Cordell, 1944, Andesite breccia dikes near Blairsden, California: Geol. Soc. America Bull., v. 55, p. 255–272.

Fenneman, N. M., 1931, Physiography of western United States: New York, McGraw-Hill Book Co., 534 p.

Ferguson, H. G., and Muller, S. W., 1949, Structural geology of the Hawthorne and Tonopah quadrangles, Nevada: U.S. Geol. Survey Prof. Paper 216, 55 p.

Fisher, R. V., 1960, Criteria for recognition of laharic breccias, southern Cascade Mountains, Washington: Geol. Soc. America Bull., v. 71, p. 127–132.

Frueh, A. J., Jr., 1958, The crystallography of silver sulfide, Ag_2S: Zeitschr. Kristallographie 110, p. 136–144.

Gianella, V. P., and Callaghan, Eugene, 1934, The earthquake of December 20, 1932, at Cedar Mountain, Nevada, and its bearing on the genesis of Basin Range structure: Jour. Geology, v. 42, no. 1, p. 1–22.

Gilluly, James, Waters, A. C., and Woodford, A. O., 1959, Principles of geology: San Francisco, Calif., W. H. Freeman and Co., 534 p.

Haas, J. L., Jr., 1971, The effect of salinity on the maximum thermal gradient of a hydrothermal system at hydrostatic pressure: Econ. Geology, v. 66, p. 940–946.

Haffty, Joseph, and Riley, L. B., 1968, Determination of palladium, platinum, and rhodium in geologic materials by fire assay and emission spectrography: Talanta, v. 15, no. 1, p. 111–117.

Hewett, D. F, and Radtke, A. S., 1967, Silver-bearing black calcite in western mining districts: Econ. Geology, v. 62, no. 1, p. 1–21.

Jackson, E. D., 1960, X-ray determinative curve for natural olivine of composition Fo_{80-90}, *in* Geological Survey research 1960: U.S. Geol. Survey Prof. Paper 400–B, p. B432–B434.

Keith, W. J., 1972, Preliminary geologic map of the Red Mountain mining district, Nevada: U.S. Geol. Survey open-file report, pl. 1.

Krauskopf, K. B., 1967, Introduction to geochemistry: New York, McGraw-Hill Book Co., 721 p.

Locke, Augustus, Billingsley, P. R., and Mayo, E. B., 1940, Sierra Nevada tectonic pattern: Geol. Soc. America Bull., v. 51, p. 513–539.

Longwell, C. R., 1960, Possible explanation of diverse structural patterns in southern Nevada: Am. Jour. Sci., v. 258–A (Bradley Volume), p. 192-203.

McKee, E. H., 1968, Geology of the Magruder Mountain area, Nevada–California: U.S. Geol. Survey Bull. 1251–H, 40 p.

Nockolds, S. R., and Allen, R., 1953, The geochemistry of some igneous rock series: Geochim. et Cosmochim. Acta, v. 4, p. 105–142.

Parsons, W. H., 1968, Criteria for the recognition of volcanic breccias—Review, *in* Igneous and metamorphic geology: Geol. Soc. America Mem. 115, p. 263–304.

Peacock, M. A., 1931, Classification of igneous rock series: Jour. Geology, v. 39, no. 1, p. 54–67.

Ramsdell, L. S., 1943, The crystallography of acanthite, Ag_2S: Am. Mineralogist, v. 28, p. 407–425.

Rittmann, Alfred, 1952, Nomenclature of volcanic rocks proposed for use in the catalogue of volcanoes and key-tables for the determining of volcanic rocks: Volcanol. Soc. Japan Bull., v. 12, ser. 2, p. 75–102.

Robinson, P. T., 1964, Cenozoic stratigraphy and structure of the central part of the Silver Peak Range, Esmeralda County, Nevada: California Univ., Berkeley, Calif., Ph.D. thesis, 107 p.

———1968, Silver Peak volcanic center, Esmeralda County, Nevada [abs.]: Geol. Soc. America Spec. Paper 115, p. 349–350.

———1972, Petrology of the potassic Silver Peak volcanic center, western Nevada: Geol. Soc. America Bull., v. 83, p. 1693–1708.

Robinson, P. T., McKee, E. H., and Moiola, R. J., 1968, Cenozoic volcanism and sedimentation, Silver Peak region, western Nevada and adjacent California, *in* Coats, R. R., Hay, R. L., and Anderson, C. A., eds., Studies in volcanology—a memoir in honor of Howell Williams: Geol. Soc. America Mem. 116, p. 577–611.

Schmincke, Hans-Ulrich, 1967, Graded lahars in the type sections of the Ellensburg Formation, south-central Washington: Jour. Sed. Petrology, v. 37, no. 2, p. 438–448.

Shawe, D. R., 1965, Strike-slip control of Basin-Range structure indicated by historical faults in western Nevada: Geol. Soc. America Bull., v. 76, p. 1361–1378.

Spurr, J. E., 1903, Descriptive geology of Nevada south of the fortieth parallel and adjacent parts of California: U.S. Geol. Survey Bull. 208, 229 p.

Stewart, J. H., 1967, Possible large right-lateral displacement along fault and shear zones in the Death Valley–Las Vegas area, California and Nevada: Geol. Soc. America Bull., v. 78, no. 2, p. 131–142.

Taylor, S. R., 1969, Trace element chemistry of andesites and associated calc-alkaline rocks, *in* Andesite Conf., Eugene and Bend, Oreg., 1968, Proc. (Internat. Upper Mantle Proj. Sci. Rept. 16): Oregon Dept. Geology and Mineral Industries Bull. 56, p. 43–63.

Tröger, W. E., 1952, Tabellen zur optischen bestimmung der gesteinsbildenden minerale: Stuttgart, E. Schweizerbart'sche Verlagsbuchhandlung (Erwin Nägele), 147 p.

Turner, F. J., and Verhoogen, John, 1960. Igneous and metamorphic petrology: New York, McGraw-Hill Book Co., 694 p.

Turner, H. W., 1900a, The Esmeralda Formation, a fresh-water lake deposit: U.S. Geol. Survey Ann. Rept. 21, pt. 2, p. 191–226.

———1900b, The Esmeralda Formation: Am. Geologist, v. 25, p. 168–170.

———1902, A sketch of the historical geology of Esmeralda County, Nevada: Am. Geologist, v. 29, p. 261–272.

———1909, Contribution to the geology of the Silver Peak quadrangle, Nevada: Geol. Soc. America Bull., v. 20, p. 223–264.

U.S. Weather Bureau, 1965, Climatic summary of the United States for 1951 through 1960—Nevada: U.S. Weather Bur., Climatography U.S. 86–22, 42 p.

Vance, J. A., 1969, On synneusis: Contr. Mineralogy and Petrology, v. 24, no. 1, p. 7–29.

Vance, J. A., and Gilreath, J. P., 1967, The effects of synneusis on phenocryst distribution patterns in some porphyritic igneous rocks: Am. Mineralogist, v. 52, nos. 3–4, p. 529–536.

Wright, L. A., and Troxel, B. W., 1966, Limitations on strike-slip displacement along the Death Valley and Furnace Creek fault zones, California [abs.]: Geol. Soc. America Spec. Paper 87, p. 188–189.

Yoder, H. S., Jr., and Tilley, C. E., 1962, Origin of basalt magmas—an experimental study of natural and synthetic rock systems: Jour. Petrology, v. 3, pt. 3, p. 342–532.

☆U.S. GOVERNMENT PRINTING OFFICE: 1977 - 789-025/39